

1. Report No. FHWA/TX-00/1702-5		2. Government Accession No.		3. Recipient's Catalog No.	
4. Title and Subtitle USING GROUND-PENETRATING RADAR FOR REAL-TIME QUALITY CONTROL MEASUREMENTS ON NEW HMA SURFACES				5. Report Date November 1999	
				6. Performing Organization Code	
7. Author(s) Tom Scullion and Yiqing Chen				8. Performing Organization Report No. Report 1702-5	
9. Performing Organization Name and Address Texas Transportation Institute The Texas A&M University System College Station, Texas 77843-3135				10. Work Unit No. (TRAIS)	
				11. Contract or Grant No. Project No. 0-1702	
12. Sponsoring Agency Name and Address Texas Department of Transportation Research and Technology Transfer Construction Division Section P. O. Box 5080 Austin, Texas 78763-5080				13. Type of Report and Period Covered Research: September 1997-August 1999	
				14. Sponsoring Agency Code	
15. Supplementary Notes Research performed in cooperation with the Texas Department of Transportation and the U.S. Department of Transportation, Federal Highway Administration. Research Project Title: Develop Improvements for Ground-Penetrating Radar					
16. Abstract <p>Segregation and poorly compacted longitudinal construction joints are major problems with new HMA (Hot Mix Asphalt) surface layers. These defect locations typically have higher air voids and greater permeability than the well-compacted areas of the mat. They can permit moisture to enter the lower HMA or base layers and they can initiate severe reductions in pavement life. The causes and remedies of pavement uniformity problems have been under investigation for many years. One major concern has been that there is no technology that can rapidly locate and quantify these defects. Recent research projects at the Texas Transportation Institute have demonstrated that Ground Penetrating Radar (GPR) technology has potential to assist in this area.</p> <p>This report describes a real-time GPR data acquisition and processing system called RADAR2000. GPR sends pulses of radar waves into the pavement structure and captures the reflections from the layer interfaces within the structure. From the reflection amplitudes and the time delays between peaks the RADAR2000 system computes and displays in real time a) the HMA surface dielectric, b) the base dielectric, and c) the surface thickness. For uniformly compacted HMA layers, the computed surface dielectric should be relatively constant; significant decreases have been found to be associated with high air void locations. The surface dielectric is related to the density of the HMA layer and can be converted to air voids content by the use of calibration cores. The base dielectric can also be converted to base moisture content by the use of laboratory generated calibration curves.</p> <p>The RADAR2000 system is demonstrated on two new construction projects. The first project involves an evaluation of two different HMA mixes placed on IH 20 in the Odessa District. The GPR data indicated that both materials contained segregated areas. The second project was newly constructed flexible pavement with a thin HMA surface layer. This section was performing poorly after only a few days in service. The GPR indicated that part of the problem was a poorly compacted longitudinal joint which was permitting moisture to enter the granular base layer. The air void content close to the joint was twice that found in the well-compacted areas of the mat.</p>					
17. Key Words Ground-Penetrating Radar, GPR, Quality Control, HMA, Asphalt Surfaces, QA/QC			18. Distribution Statement No restrictions. This document is available to the public through NTIS: National Technical Information Service 5285 Port Royal Road Springfield, Virginia 22161		
19. Security Classif.(of this report) Unclassified		20. Security Classif.(of this page) Unclassified		21. No. of Pages 54	22. Price

**USING GROUND-PENETRATING RADAR FOR REAL-TIME
QUALITY CONTROL MEASUREMENTS ON NEW HMA SURFACES**

by

Tom Scullion
Associate Research Engineer
Texas Transportation Institute

and

Yiqing Chen
Assistant Research Scientist
Texas Transportation Institute

Report 1702-5
Project Number 0-1702
Research Project Title: Develop Improvements for Ground-Penetrating Radar

Sponsored by the
Texas Department of Transportation
In Cooperation with the
U.S. Department of Transportation
Federal Highway Administration

November 1999

TEXAS TRANSPORTATION INSTITUTE
The Texas A&M University System
College Station, TX 77843-3135

DISCLAIMER

The contents of this report reflect the views of the authors, who are responsible for the opinions, findings, and conclusions presented herein. The contents do not necessarily reflect the official view or policies of the Texas Department of Transportation (TxDOT). This report does not constitute a standard, specification, or regulation, nor is it intended for construction, bidding, or permit purposes. The engineer in charge of the project was Tom Scullion, P.E. #62683.

There is no invention or discovery conceived or first actually reduced to practice in the course of or under this contract, including any art, method, process, machine, manufacture, design, or composition of matter, or any new and useful improvement thereof, or any variety of plant, which is or may be patentable under the patent laws of the United States of America or any foreign country.

ACKNOWLEDGMENTS

This project is part of TxDOT's continuing interest in applying GPR technology to a range of pavement problems. This work would not be possible without the support and direction provided by Mr. Carl Bertrand of the Design Division, Pavement Section. Funding was provided by both TxDOT and the Federal Highway Administration.

TABLE OF CONTENTS

	Page
LIST OF FIGURES	viii
CHAPTER 1. INTRODUCTION	1
1.1. BASICS OF GROUND-PENETRATING RADAR	1
1.2. GPR REFLECTIONS FROM THIN SURFACINGS	3
1.3. COMPUTATION OF LAYER THICKNESSES AND DIELECTRICS	7
1.4. RELATIONSHIP OF COMPUTED LAYER DIELECTRICS TO ENGINEERING PROPERTIES	9
CHAPTER 2. DESCRIPTION OF RADAR2000	17
CHAPTER 3. CASE STUDIES	27
CASE STUDY 1 SEGREGATION STUDIES ON IH 20	27
CASE STUDY 2 POORLY COMPACTED LONGITUDINAL CONSTRUCTION JOINT	34
CHAPTER 4. CONCLUSION AND RECOMMENDATIONS	41
REFERENCES	43

LIST OF FIGURES

Figure	Page
1. GPR Equipment and Principles of Operation	2
2. Typical GPR Return Signal from Flexible Pavement with a Thin Overlay	4
3. Typical GPR Reflection from a Newly Constructed Pavement Consisting of a Thick Granular Base and Thin Surfacing	6
4. Correlation Between Dielectric Value and Gravimetric Moisture Content of Texas Aggregates (Saarenketo and Scullion, 1995)	13
5. Lab Procedure and Model Proposed to Relate Base Dielectric and Moisture Content	14
6. Laboratory Test Results Relating Air Void Content of HMA Samples to Measured Dielectric Values (Saarenketo, 1996)	15
7. Introduction Screen to RADAR2000	18
8. Main Set-Up Screen for RADAR2000	19
9. Display During Data Acquisition	21
10. Real-Time Display of HMA Thickness and Layer Dielectrics	22
11. Options Screen from RADAR2000	25
12. Real-Time Display of HMA Thickness, HMA Air Voids, and Base Moisture Content .	26
13. Lay Down Operation Large Stone Superpave Mix on IH 20	29
14. Evidence of Visual Segregation in Type B Material (One Week After Placement)	30
15. Typical GPR Trace from Superpave Inlay on IH 20, Odessa	31
16. Surface Dielectric Plots for Superpave vs. Type B Materials (Computed Surface Dielectric vs. Distance)	32
17. Summary GPR Results from Type B Material	33
18. Forensic Evaluation on IH 20	35
19. GPR Results Taken Over Longitudinal Construction Joint on IH 20	36

LIST OF FIGURES (Continued)

Figure	Page
20. Laboratory Calibration Curve for the Base Material, Dielectric, as Measured with the Adek Probe, to the Moisture Content	38
21. Using the Lab Calibration Factors to Estimate HMA Air Void and Base Moisture Content for IH 20	39

CHAPTER 1. INTRODUCTION

1.1. BASICS OF GROUND-PENETRATING RADAR

The Texas Transportation Institute's Ground-Penetrating Radar (GPR) unit is shown in Figure 1(a). This system sends discrete pulses of radar energy into the pavement system and captures the reflections from each layer interface within the structure. This particular GPR unit operates at highway speed (60 mph), transmits and receives 50 pulses per second, and can effectively penetrate to a depth of 2 feet. A typical plot of captured reflected energy versus arrival time for one pulse is shown in Figure 1(b), as a graph of volts versus time in nanoseconds.

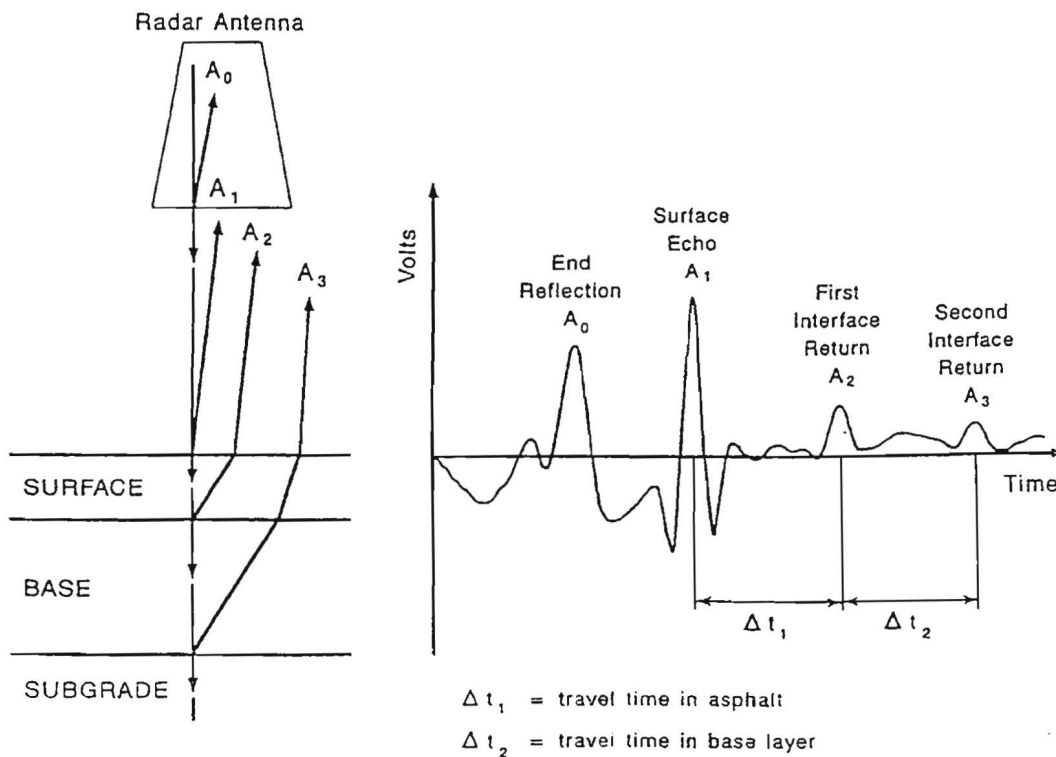
In Figure 1(b), the reflection A_1 is the energy reflected from the surface of the pavement and A_2 and A_3 are from the top of the base and subgrade respectively. As described in Section 1.3, these amplitudes of reflection and the time delays between reflections are used to calculate both layer dielectrics and thickness. The dielectric constant of a material is an electrical property which is most influenced by moisture content and density. If the moisture content for a layer increases, then the dielectric of the layer will increase which will result in an increase in the energy reflected from the top of the layer. An increase in air voids would have the opposite effect if the amount of air in a layer increases the energy reflected and the resulting dielectric would decrease.

TTI has established a range of typical dielectrics for most paving materials. For example HMA layers normally have a dielectric value between 4.5 and 6.5, depending on the coarse aggregate type. Measured values significantly higher than this would indicate the presence of excessive moisture. Lower values could indicate a density problem or indicate that an unusual aggregate, such as lightweight, had been used.

The examples below illustrate how changes in materials properties and structure would influence the typical GPR trace shown in Figure 1.



(a) TTI GRP Equipment.



(b) Principles of Ground-Penetrating Radar. The incident wave is reflected at each layer interface and plotted as return voltage against time of arrival in nanoseconds.

Figure 1. GPR Equipment and Principles of Operation.

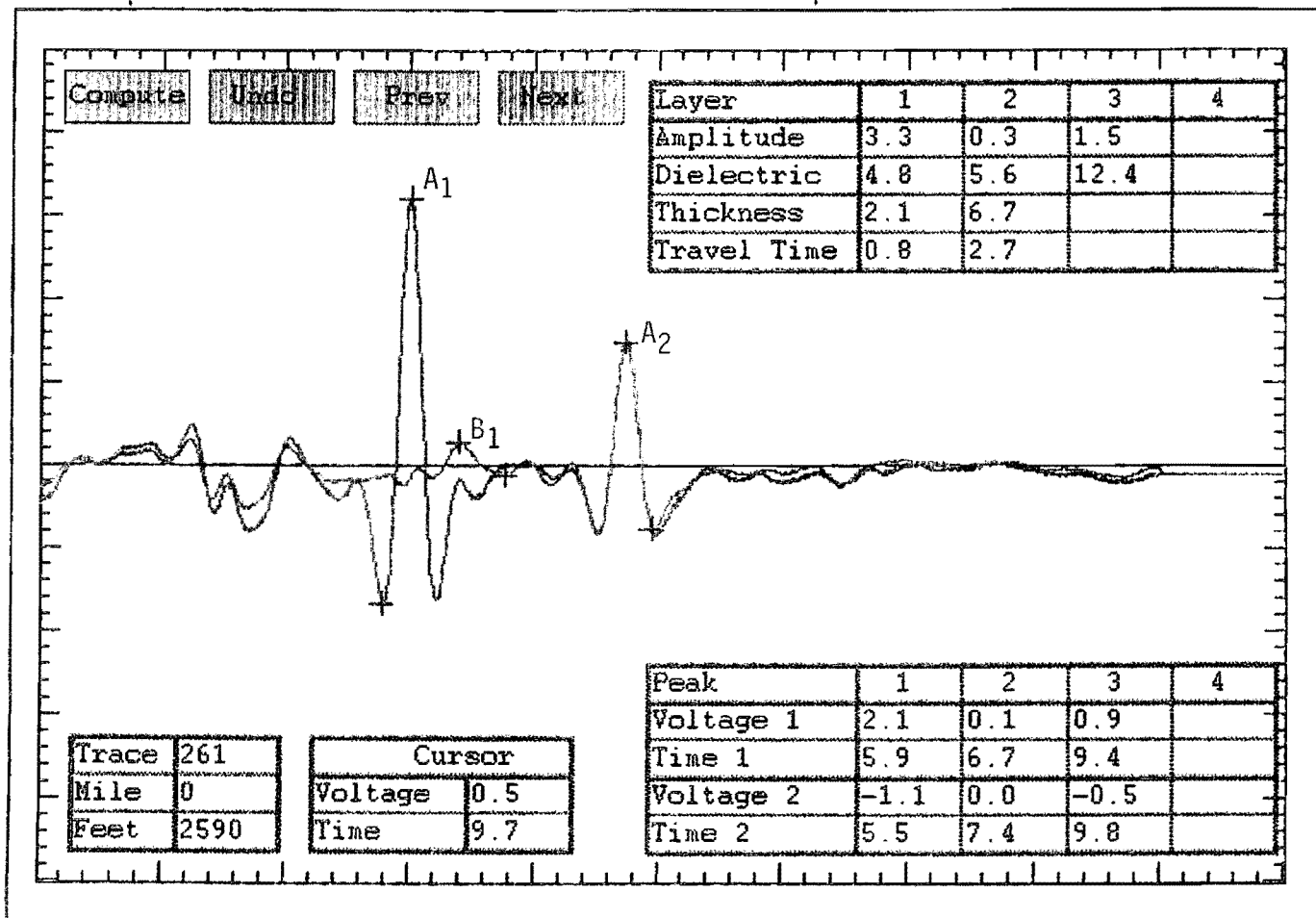
- 1) If the thickness of the surface layer increases, then the time interval between A_1 and A_2 would increase.
- 2) If the base layer becomes wetter, then the amplitude of reflection from the top of the base A_2 would increase.
- 3) If there is a significant defect within the surface layer, then a reflection will be observed between A_1 and A_2 . This could be either a positive reflection for trapped moisture or a negative reflection for stripping.
- 4) As the unit travels along the highway it collects traces at regular intervals. Therefore, GPR has the potential to monitor the uniformity of the surfacing layer. Large changes in the surface reflection A_1 would indicate changes in either the density (decrease in amplitude) or moisture content (increase in amplitude) along the section.

1.2. GPR REFLECTIONS FROM THIN SURFACINGS

Reflections from thin layers present a problem for 1 GHz GPR systems because the reflections from the top and bottom of the layer overlap. This section will describe a special signal processing techniques that has been developed to handle this problem. The cases presented below describe how to perform GPR signal processing on two typical thin HMA layers.

Case 1 HMA Overlay (Thin HMA Over an Existing HMA Surface)

Figure 2 contains a single GPR reflection from one location on a flexible pavement containing a new 1.5-inch overlay. The blue line in Figure 2 represents the raw data. As before, A_1 and A_2 are reflections from the top of the HMA and top of the base layer. With GPR systems operating at a frequency of 1 GHz, one complicating issue is that reflection from layers less than 3 inches thick will overlap and make it impossible to detect and measure the true layer interface reflection without additional signal processing. As the pavement in Figure 2 had a recent thin overlay, the reflection from the surface is partially merged with that from the top of the old HMA layer. A surface de-convolution (subtraction) technique has been developed to handle this situation;



Reflections A₁, B₁, A₂ from surface, bottom of overlay, top of flexible base, respectively. This is viewed as the "Ideal" Case 1, well bonded overlay no defects in lower HMA. The blue line is raw GPR return signal, the red line is obtained after surface removal.

Figure 2. Typical GPR Return Signal from Flexible Pavement with a Thin Overlay.

this technique has been described elsewhere (Scullion, Chen, and Lau 1992). It effectively removes the surface reflection from the trace and leaves the reflections from the lower pavement interfaces. The subtraction technique has been applied to the GPR reflection shown in Figure 2. The blue line represents the original captured reflection from the pavement structure, after the surface removal technique is applied, the red line is obtained. Reflection B_1 clearly shows the reflection from the top of the old HMA layer.

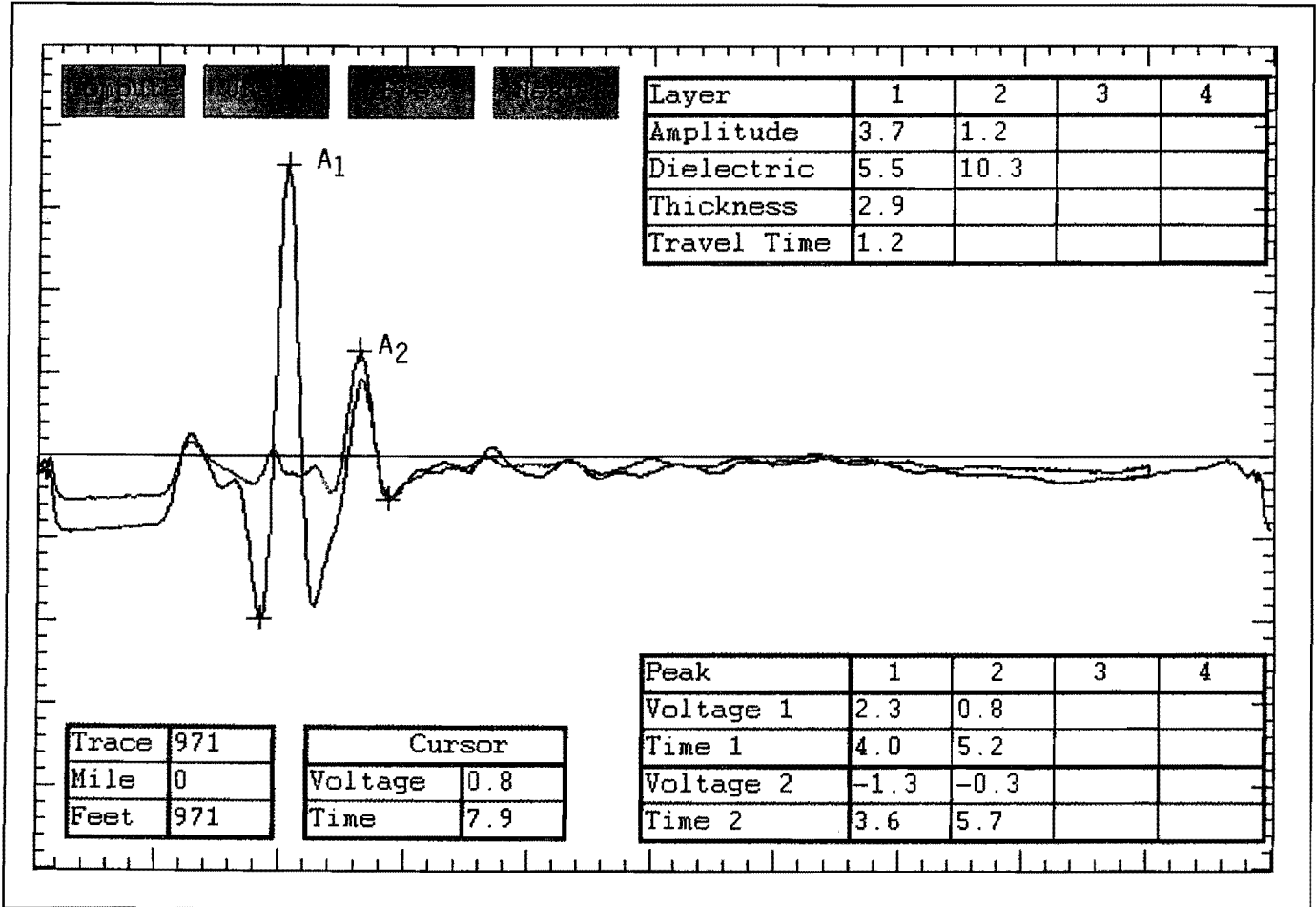
One point that must be emphasized is that GPR only works if there is an electrical contrast between pavement layers. If two layers have similar electrical properties and are bonded together, then there will be little energy reflected from that interface, and it will be impossible to detect the interface in the reflected signal. This condition is the case with thick asphalt stabilized bases constructed with several lifts of identical material. It is often difficult to see interfaces within homogeneous layers. With these pavements, a significant interface reflection within the layer would be a cause for concern. With a new thin HMA overlay placed over an existing flexible pavement sufficient contrast often exists between the old and new asphalt layers to provide a small reflection from the interface.

The trace shown in Figure 2 is classified as an ideal trace for a recent thin HMA overlay placed on an existing old HMA layer. The small reflection at the interface (B_1), which is found after surface removal, indicates a small electrical contrast between the old and new HMA layers. As shown in Figure 2, the dielectric values for the upper and lower layers were computed to be 4.8 and 5.6, respectively, which are considered to be normal. The thickness of the overlay was computed to be 2.1 in and the old HMA layer to be 6.7 in. There are no strong reflections in the lower HMA layer between B_1 and A_2 ; therefore, this layer is judged to be homogeneous and defect free, and it should be possible to extract a solid core from this location. The dielectric from the top of the flexible base was calculated to be 12.4, which is classified as marginal for granular material. Top-quality flexible base materials have been found to have a calculated dielectric of below 10, and saturated base layers have a value greater than 16.

Case 2 New Construction (Thin HMA Over a Granular Base)

A thin HMA layer over a granular base is a popular pavement type in Texas and one that is straightforward to process as long as the surface removal technique is applied. Figure 3 shows the

Texas Transportation Institute



Pavement data file : d:\gprdata\odessa\ih20\real3.dat
 Metal plate file : mt12.dat
 Velocity factor : 5.900 Dielectric : 6.000

Reflections A₁ and A₂ are from the surface and top of base, respectively. This scenario is the ideal case. The red line is obtained after surface removal.

Figure 3. Typical GPR Reflection from a Newly Constructed Pavement Consisting of a Thin Surfacing over a Thick Granular Base.

reflection from a thin 3 inch thick HMA layer over a thick granular base. As the base typically has significantly more moisture than the HMA, there is often a large reflection from the top of the base. As will be described later in this section, the amplitude of reflection from the top of the base is related to the moisture content of the base. However, with HMA surfacings less than 3 inches thick, the surface and base reflections overlap. Therefore in order to measure the true amplitude of reflection from the top of the base, it is necessary to use the surface removal technique described earlier. Again, the blue line is the raw data and the red line represents the reflections remaining after the surface is removed.

The RADAR2000 software described later in this report automatically applies this surface removal technique for pavements with thin surface layers.

1.3. COMPUTATION OF LAYER THICKNESSES AND DIELECTRICS

Maser and Scullion (1991) described the principles of GPR data processing for highways. By automatically monitoring the amplitudes and time delays between peaks, it is possible to calculate layer dielectrics, layer thickness, and to estimate the moisture content of granular base material. These equations are summarized below (see Maser and Scullion, 1991 for derivations).

$$\sqrt{\epsilon_a} = \frac{A_m}{A_1} \frac{A_1}{A_m} \quad (1)$$

where

ϵ_a = the dielectric of the surface layer

A_1 = the amplitude of reflection from the HMA surface in volts

A_m = the amplitude of reflection from a large metal plate in volts (this represents the 100% reflection case)

$$h_1 = \frac{c \times \Delta t_1}{\sqrt{\epsilon_a}} \quad (2)$$

where

$h_1 =$ the thickness of HMA layer

$c =$ the speed of travel of a GPR wave in free space (ins/ns) as measured by the system. For two-way travel this value should be approximately 5.9 inches per nanosecond, the speed of an electromagnetic wave in a vacuum. The speed as measured by the GPR unit can be computed using the height calibration procedures described in (Scullion, Lau, and Chen, 1992)

$\Delta t_1 =$ the travel time in the HMA layer in nanoseconds

$$\sqrt{\epsilon_b} = \sqrt{\epsilon_a} \left[\frac{1 - \left[\frac{A_1}{A_m} \right]^2 - \left[\frac{A_2}{A_m} \right]}{1 - \left[\frac{A_1}{A_m} \right]^2 - \left[\frac{A_2}{A_m} \right]} \right] \quad (3)$$

where

$\epsilon_b =$ the dielectric of the base layer

$A_2 =$ the amplitude of reflection from the top of the base layer in volts

Using the amplitude and time delay data shown in Figure 3, ($A_1 = 3.7$ volts, $A_2 = 1.3$ volts, $\Delta t_1 = 1.2$ nanoseconds, and given $A_m = 9.14$ volts), it is possible to calculate the following dielectrics and layer thicknesses:

Using Equation 1,

$$\sqrt{\epsilon_a} = \frac{A_m + A_o}{A_m - A_o} = \frac{9.14 + 3.7}{9.14 - 3.7} = 2.36$$

$$\epsilon_a = 5.5$$

Using Equation 2,

$$h_1 = \frac{5.9 \times \Delta t_1}{\sqrt{\epsilon_a}} = \frac{5.9 \times 1.2}{2.36} = 3.0 \text{ ins}$$

Using Equation 3,

$$\sqrt{\epsilon_b} = 2.36 \left[\frac{1 - \left(\frac{3.7}{9.14} \right)^2 - \left(\frac{1.2}{9.14} \right)}{1 - \left(\frac{3.7}{9.14} \right)^2 - \left(\frac{1.2}{9.14} \right)} \right]$$

$$= 3.23$$

$$\epsilon_b = 10.4$$

The layer dielectrics and thickness computed by the automated data processing system are shown in the box in the upper right hand corner of Figure 3. The slight differences with those values calculated above is attributed to rounding errors.

1.4. RELATIONSHIP OF COMPUTED LAYER DIELECTRICS TO ENGINEERING PROPERTIES

The engineering properties of most interest to highway engineers are the air void content of the HMA layer and the moisture content of the granular base layer. Both impact the computed layer dielectric. The computed dielectric for any layer is a function of the volumetric ratios of the components and their individual dielectric values. For example, the major components of a dry HMA layer are aggregate, asphalt, and air. For a granular base the components are aggregate, air, and moisture. The typical component dielectrics are tabulated below:

Material	Dielectric
Air	1.0
Water	81.0
Aggregate	5.5 (range 4 to 8 depending on rock type)
Asphalt	2.2

Therefore, the addition of air to a HMA surface will cause a significant reduction in that layer's dielectric value. Consequently, the addition of moisture to a granular base layer will cause a significant increase in its dielectric value. A surface and base dielectric plot can be computed from the collected GPR data as the vehicle passes over a newly constructed HMA layer. As shown later in this report, significant changes in either the surface or base dielectric should be cause for concern.

Relationship Between Base Dielectric and Moisture Content

Since the late 1980s the Texas Transportation Institute and other agencies have investigated the relationship between dielectric and engineering properties of highway materials. Halabe et al. (1989) applied the Complex Refractive Model (CRIM) to study the relationship between the dielectric of a mixture and the volumetric ratios and dielectric properties of the components. For a granular base layer the model is shown below:

$$\sqrt{\epsilon_b} = \sum v_i \sqrt{\epsilon_i} \quad (4)$$

where

ϵ_b = relative dielectric constant of the base layer

v_i = volume fraction of component i

ϵ_i = relative dielectric constant of component i

The components of the base material are solid particles, water, and air. The dielectric constants of water and air can be taken as 81 and 1, respectively.

In order to determine the base moisture content from this model, one has to assume both the Bulk density of the material and the dielectric constant of the solids. Once these assumptions are made, the moisture content (% by total wt.) can be computed from equations (1) and (4) making various substitutions for porosity and percent saturation in terms of bulk density to obtain the following:

$$\% \text{ Moisture Content} = \frac{\sqrt{\epsilon_b} - 1}{\sqrt{\epsilon_b} + 1} \frac{\gamma_d / \gamma_s (\sqrt{\epsilon_s} + 1)}{\gamma_d / \gamma_s (\sqrt{\epsilon_s} - 22.2)} \quad (5)$$

where

- ϵ_b = base dielectric constant (determined from eq. 3)
- ϵ_s = solids dielectric constant (varies from 4 to 8 depending on source material)
- γ_d = dry density (lbs./ft³)
- γ_s = density of solids (~165 lbs./ft.³)

Studies conducted by the Texas Transportation Institute in the early 1990s used this model to determine the moisture content of a granular base layer (Maser and Scullion, 1991). In these studies a sample of the base was taken at one location to measure its dry density. This estimate was then treated as constant in the computation of moisture contents at other locations. A Root Mean Square error between measured and predicted moisture content of less than 2% was reported from these initial studies. The assumption that the dry density was constant throughout the project produced errors.

In 1995, Scullion, Chen, and Lau proposed an alternate approach to computing base moisture content from GPR data. Their approach involved generating a laboratory calibration curve for any granular base material. This calculation can now be performed as a standard feature of the traditional optimum moisture content procedure, where samples are molded at a range of moisture contents to determine their maximum density. A dielectric probe manufactured by Adek, Ltd. (Plakk, 1994) is used to measure the surface dielectric of the sample as part of this process. In the mid 1990s a series of tests was conducted on a range of base materials from around Texas (Saarenketo and Scullion,

1995, 1341-2). Typical results from those studies are shown in Figure 4. Figure 4(a) shows the relationship between dielectric value and moisture content for a group of similar aggregates (all limestone); for this group the relationship is similar for each aggregate type. This outcome is not the case in the lower graph, Figure 4(b), which presents results from a range of different aggregates. The main conclusions from these studies are 1) an increase in the base moisture will cause an increase in base dielectric, and 2) this relationship between base moisture content and dielectric is unique for each material type.

The laboratory calibration approach described above has been built into the RADAR2000 software. The user inputs the relationship between base moisture content and base dielectric, using the procedure and model shown in Figure 5. This model assumes that the relationship will have two linear portions, each defined by a slope and intercept.

Relationship Between Surface Dielectric and HMA Air Voids

In the early 1990s several major studies were conducted in Finland to investigate the use of GPR for quality control measurements on new HMA surfaces, (Saarenketo, 1996, Saarenketo and Roimela, 1998). As part of these studies, a laboratory test was performed to relate the HMA surface dielectric measured with the Adek probe to the air void content. The researchers performed tests on both laboratory molded and field samples. Figure 6 shows a typical set of results from the laboratory samples. There is substantial scatter in this data but it is noted that the results are for a range of mixes with different aggregate types. The work of the Finnish researchers found that the exponential relationship shown in Figure 6 ($\% \text{ air voids} = A \times \exp. [-B \times \text{surface dielectric}]$) was reasonable for both field and lab samples.

RADAR2000 adopts this exponential relationship to permit the user to convert the surface dielectric as measured by the GPR to HMA air voids content. It is proposed that the constants A and B be determined for each material type. This determination requires taking a minimum of two calibration cores from each project in locations where the surface dielectric has been measured with GPR. A laboratory air void determination is then made on the cores. Knowing the computed field dielectrics and lab air voids at two locations, the values of A and B can be computed. Case Study 2 demonstrates the computation of A and B later in this report.

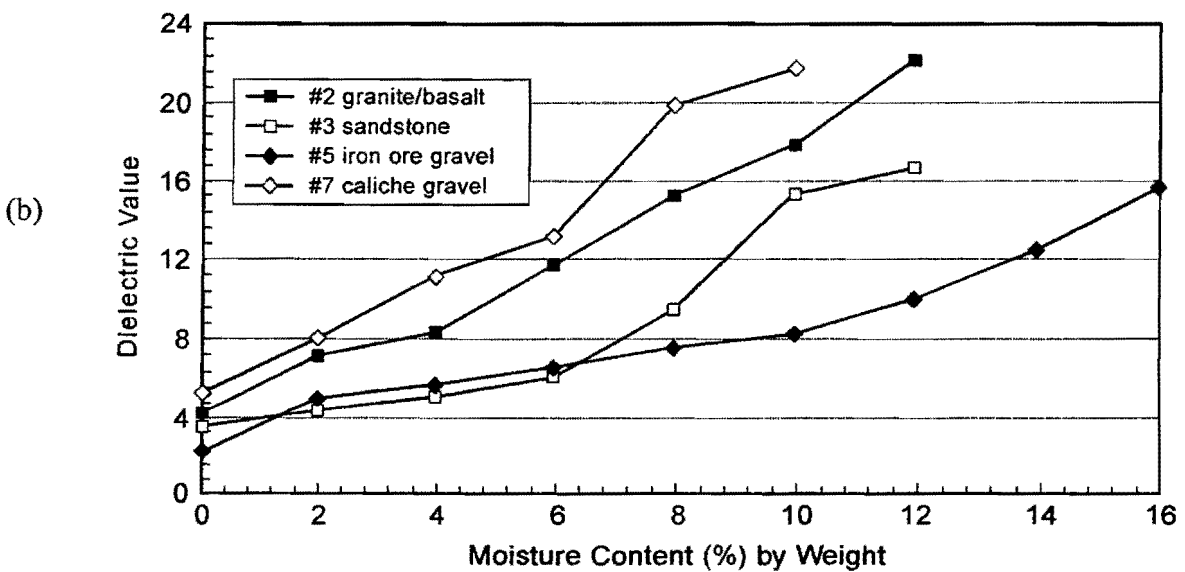
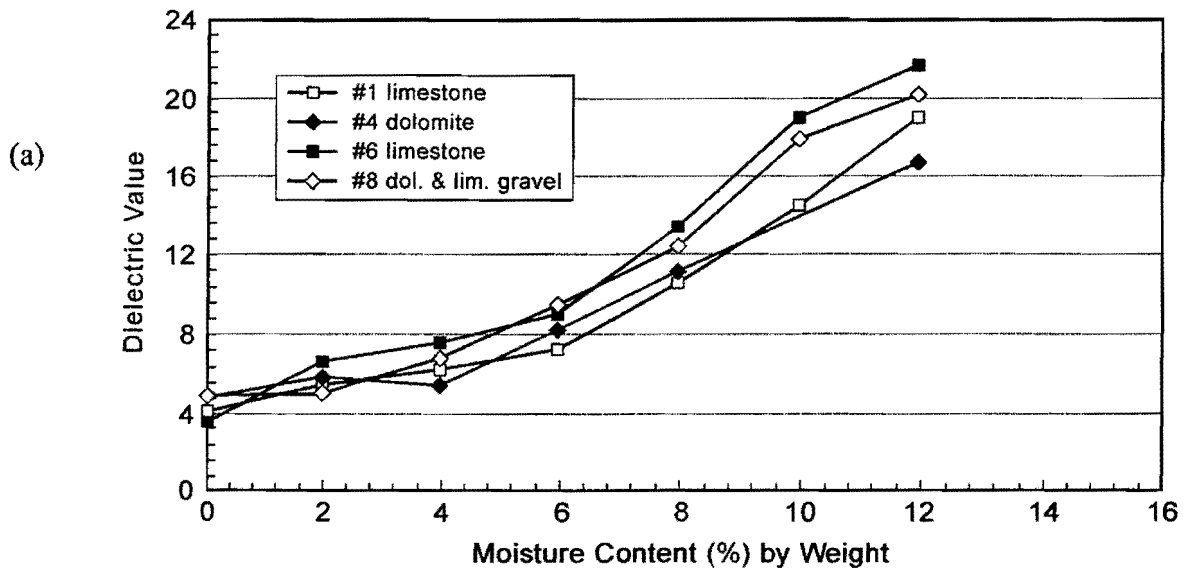
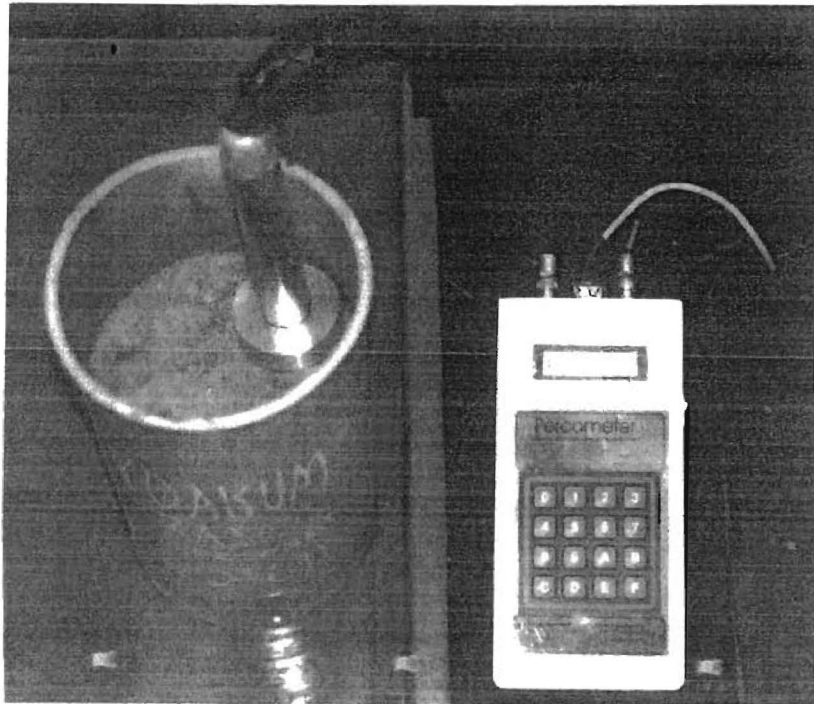
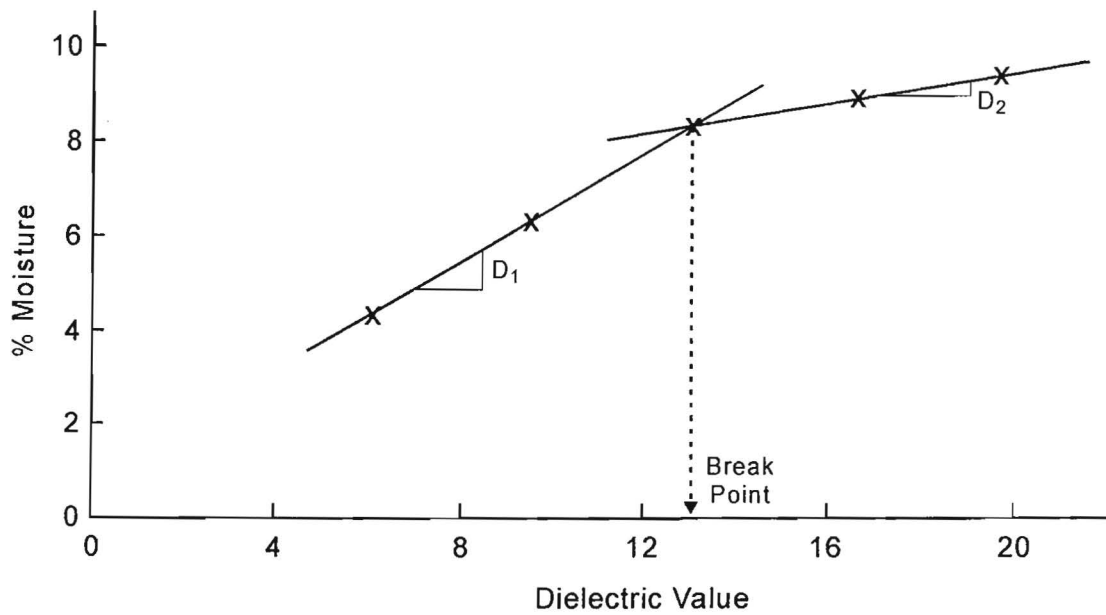


Figure 4. Correlation Between Dielectric Value and Gravimetric Moisture Content of Texas Aggregates (Saarenketo and Scullion, 1995).



(a) Laboratory dielectric test



(b) Model use to relate dielectric to base moisture content

Figure 5. Lab Procedure and Model Proposed to Relate Base Dielectric and Moisture Content.

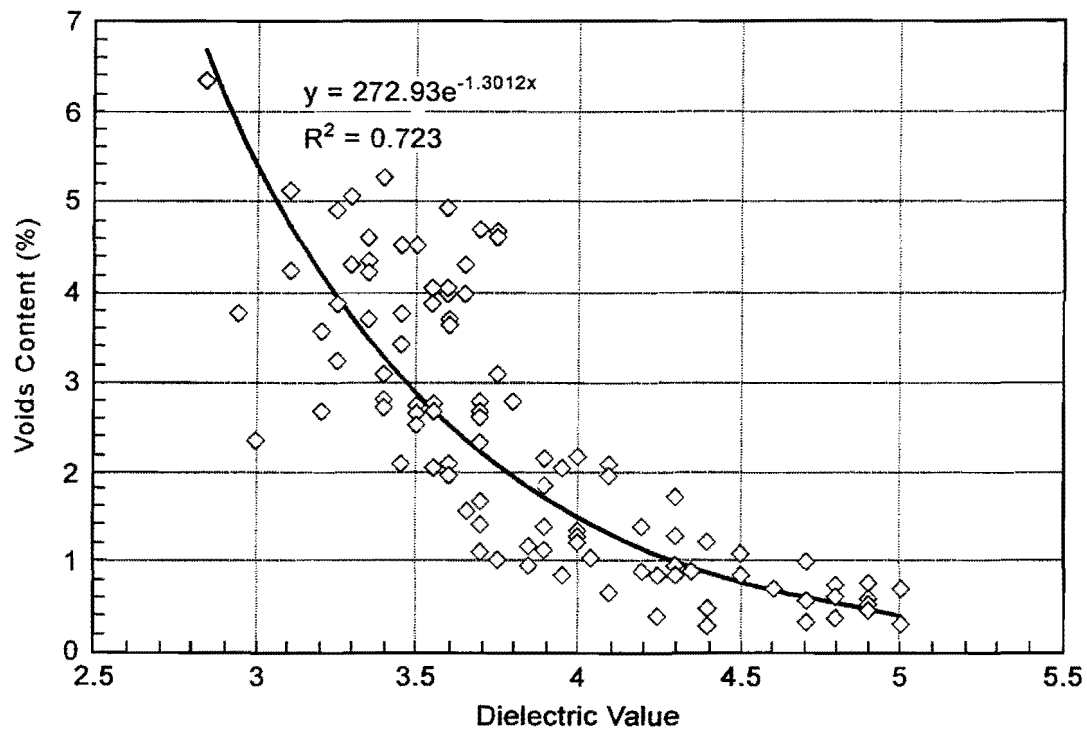


Figure 6. Laboratory Test Results Relating Air Void Content of HMA Samples to Measured Dielectric Values (Saarenketo, 1996).

CHAPTER 2. DESCRIPTION OF RADAR2000

RADAR2000 is the latest GPR data acquisition system developed by the Texas Transportation Institute for the Texas Department of Transportation. It can be used for both network and project-level GPR investigations. A unique feature of this package is that, for the first time, it provides substantial real-time data processing capabilities. This feature is intended for use with QC/QA assessments of new HMA surfaces. In the QC/QA mode the system can capture, process, and display results from GPR data collected at 1 foot spacings while traveling at 20 mph. For network-level data acquisition, without processing, the system captures GPR traces at highway speeds.

RADAR2000 is fully Windows 98 compatible. The main screens from this system are shown in Figures 7 through 12, each described below:

Figure 7: Introduction Screen to RADAR2000

The first screen displayed contains information about the antenna used to perform the test as well as the last calibration date. This screen is not changed under normal operations.

Figure 8: Main Setup Screen for RADAR2000

The main setup screen for the RADAR2000 software. On this screen, the user inputs project information in the Header box and then enters other key items as follows:

- Open File The user defines an output file name.
- Distance/Time Specifies the data collection mode as either distance or time based.
- Ms/Trace Specifies the time or distance between traces.
- Monitor/Collect Monitor permits the user to display GPR traces without storing; Collect has both display and storage options.
- Monitor Data This permits the user to go to the next screen to start data acquisition.
- Playback Review previously collected GPR traces.

Meta Initialization

TTI *RADAR 2000* TxDoT

Radar Manufacturer:

Radar Model # / Serial #:

Program Version:

Vehicle ID:

Velocity Factor Calibration Date:

Short-term Stability Test Date:

Long-term Stability Test Date:

Distance Calibration Date / Factor:

Comments:

Operator:

Next...

Figure 7. Introduction Screen to RADAR2000.

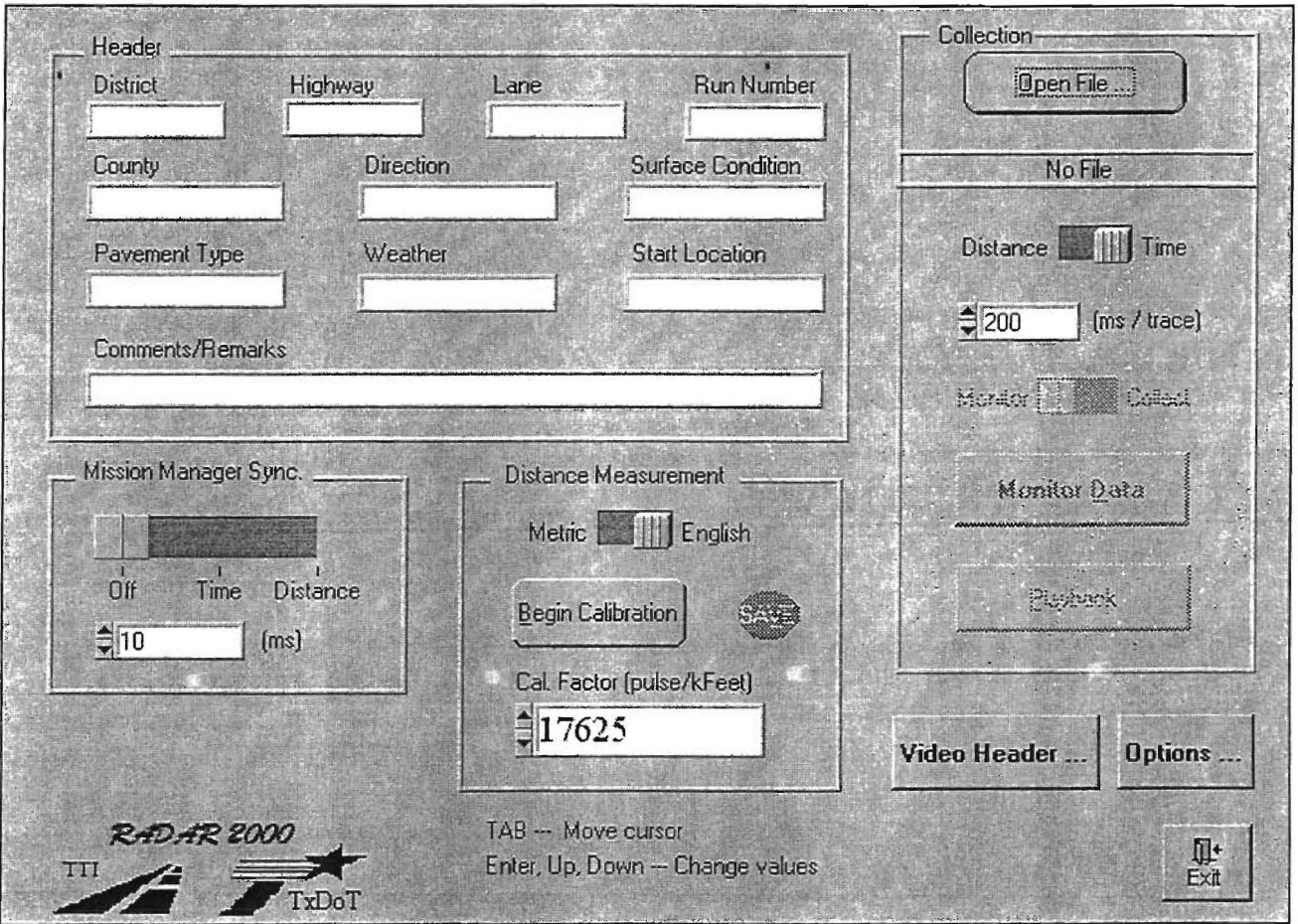


Figure 8. Main Setup Screen for RADAR2000.

- Options Described in Figure 11.
- Begin Calibration Permits the user to calculate a distance calibration factor. The vehicle is driven a known distance and the factor is automatically calculated and stored.
- Metric/English Provides the capability of collecting distance data in either English or metric units.

Figure 9: Display During Data Acquisition

Once the user selects the Monitor or Collect function in Figure 8, the system starts collecting GPR traces at the specified distance or time interval. As shown in Figure 9, the system displays the individual raw GPR reflections as a graph of volts versus time. The distance information for the displayed trace is shown at the top of the figure. In this case, the trace was collected 11 feet from the start of data collection, with a data collection interval of one trace per foot. These traces, together with the distance information, are stored in the output file for post processing.

Figure 10: Real-Time Display of HMA Thickness and Layer Dielectrics

Pressing the F1 key during data acquisition will activate the real-time data processing function of RADAR2000 as shown in Figure 10. Each one of the displays is described below:

- Upper Left (GPR Trace and Processing Window)
This box displays the GPR trace being collected at that location (412 feet from the start). The software automatically applies the surface subtraction routine described earlier so that superimposed on the raw data trace is the same trace with the surface echo removed. To assist the peak tracking function the user manually defines the location of the reflection from the second layer, the range limits are the two vertical lines shown in this box. The user can manually reposition these limits by using the arrow keys. The software then tracks the peak surface reflection and the reflection

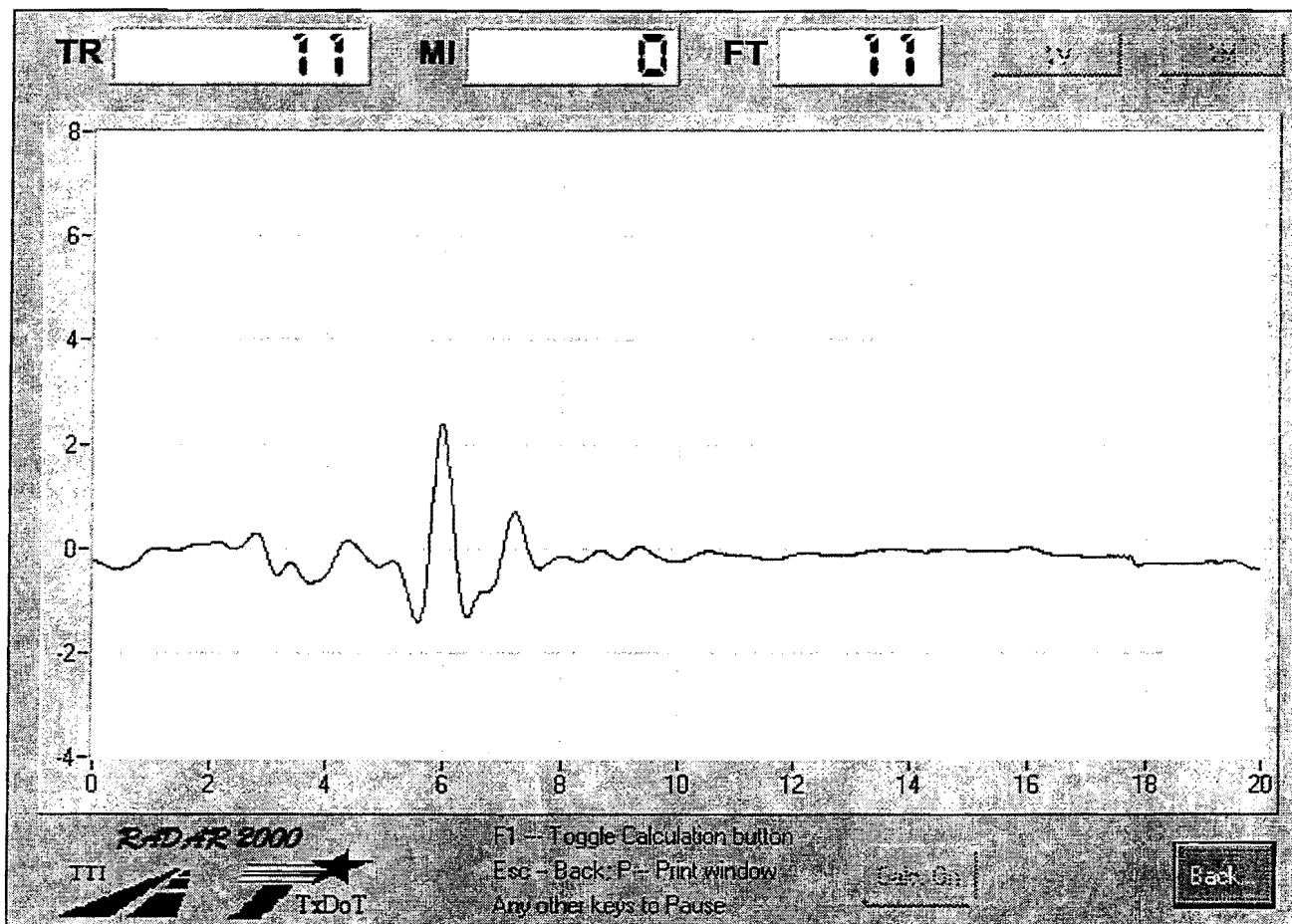
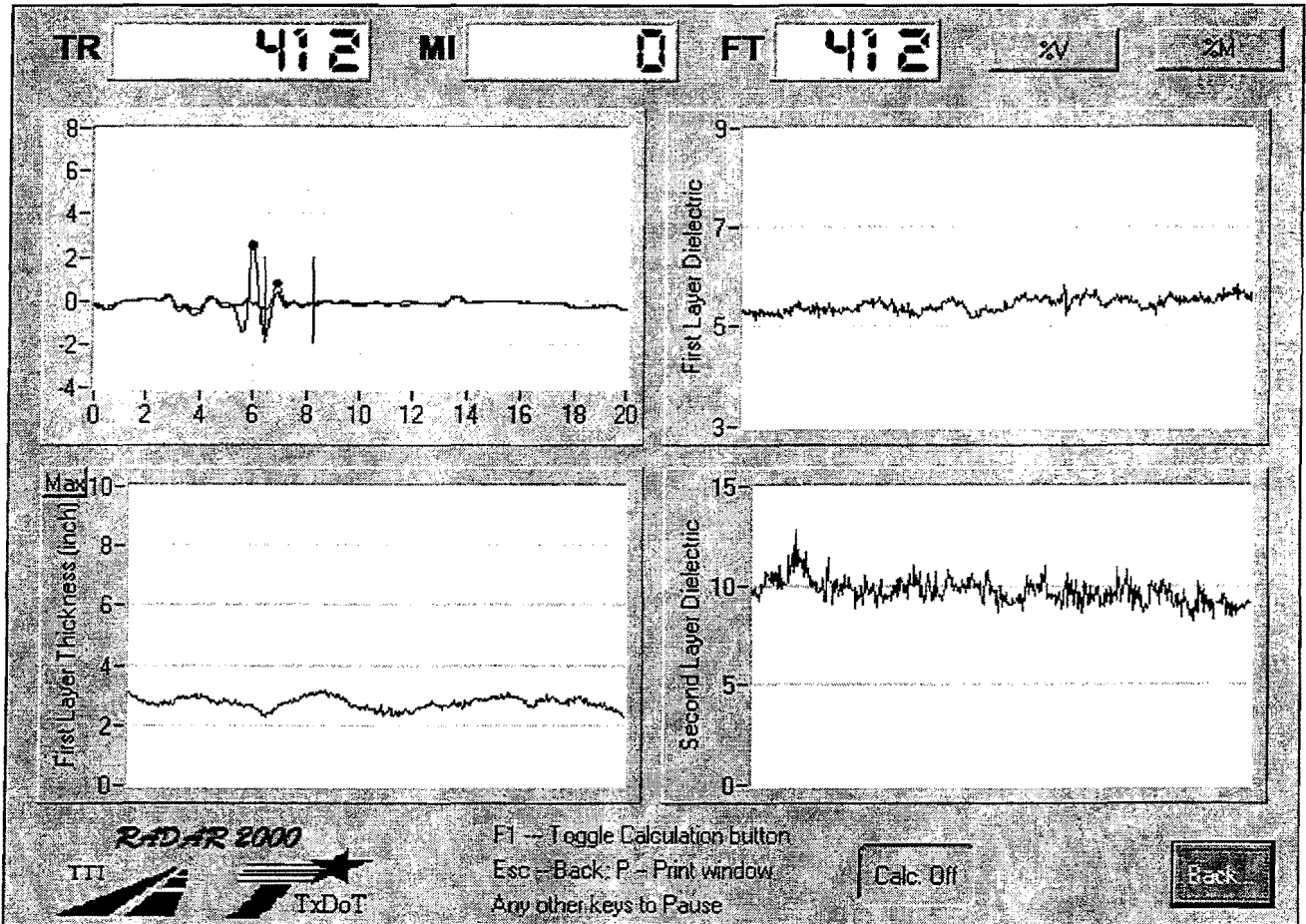


Figure 9. Display during Data Acquisition.



- Upper Left: Actual Trace
- Upper Right: Computer Surface Dielectric
- Lower Left: Computed Top Layer Thickness
- Lower Right: Computed Base Dielectric

Figure 10. Real-Time Display of HMA Thickness and Layer Dielectrics.

from the top of the second layer. The system places a dot on the peaks it has located. The software then automatically calculates the amplitudes of reflection and the time delay between peaks in order to compute the surface layer thickness and layer dielectrics using the equations discussed earlier in this report. These values are then displayed in the other three graphs shown in this figure. The remaining graphs scroll across the page showing processed results for the entire section.

- Upper Right (First Layer Dielectric)

RADAR2000 calculates the surface dielectric from the amplitude of surface reflection using Equation 1. The newly calculated value for this location is plotted at the right of the figure. The graph scrolls providing a real-time plot of the computed surface dielectric as the vehicle travels along the pavement. This graph is key to identifying problems with surface density. For homogeneous well-compacted materials, this graph should be a horizontal line. A small amount of noise is typical for most materials, but significant localized reductions in surface dielectric are cause for concern. These results can only be explained by reductions in HMA density. Reductions in dielectric greater than 0.5 are highly significant.

- Lower Left (First Layer Thickness in Inches)

The surface layer dielectric together with the time delay between peaks are used in Equation 2 to calculate the thickness of the top layer. This graph scrolls across the screen with the most recent thickness at the right of the figure.

- Lower Right (Second Layer Dielectric)

RADAR2000 uses Equation 3 to calculate the dielectric of the second layer in the structure. For overlays, the second layer will be the top of the old HMA layer. For new construction, the second layer is often the top of the flexible base layer. The dielectric of the flexible base layer is directly related to the moisture content of the layer. Significant increases in dielectric would be a cause for concern. For premier materials, a dielectric value below 10 is recommended; materials with poor strength characteristics and poor resistance to freeze thaw cycling will have a dielectric value greater than 16.

Figure 11: Options Screen for RADAR2000 Including Laboratory Calibration Factor

In this Options screen, the user provides the name of the metal plate file to be used in data processing as well as the laboratory determined calibration factors needed to convert the surface and base dielectrics into surface density and base moisture content

Once the metal plate file has been opened, the metal plate amplitude computed for the first trace in the file is displayed in the Amplitude box. The Window box defines the start position of the markers for detecting the reflection from the second layer, these represent the two vertical lines in Figure 10. The Template Subtraction button is used to activate the option that automatically removes the surface reflection prior to data processing.

The user inputs the laboratory calibration factors, used to convert computed dielectrics to engineering properties, in the other boxes as described below:

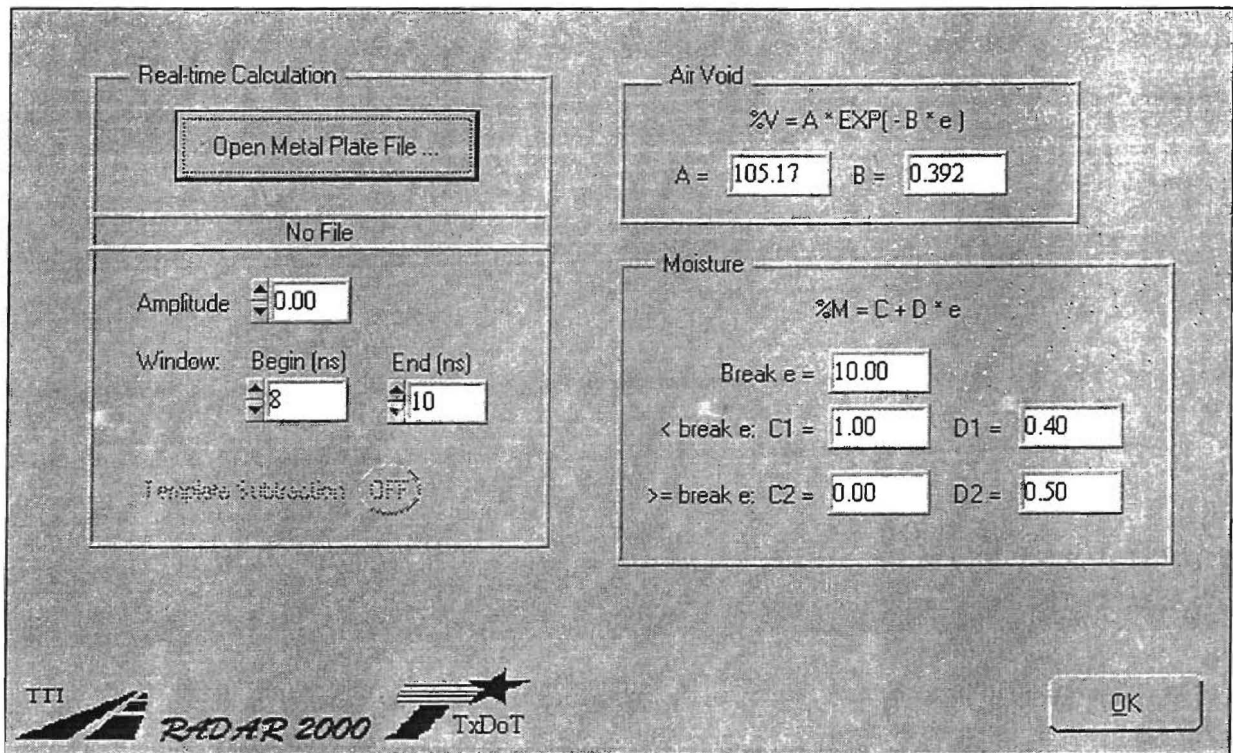
- Air Voids (A and B)

During GPR data collection a minimum of two locations is identified for calibration coring. These locations should contain significantly different layer dielectrics. Cores are taken and returned to the laboratory for air void determination. When two cores are taken, a simple spreadsheet can be used to compute the constants A and B as defined in Figure 6. If more than two cores are taken then linear regression techniques can be used to obtain A and B.

- Base Moisture Content (C and D)

Laboratory testing on base materials from around Texas has shown that the relationship between base moisture content and base dielectric is not linear. The relationship is sometimes curvilinear and often the base dielectric increases steeply above a certain moisture content. As described in Figure 5, the RADAR2000 system assumes that this relationship can be approximated as two straight lines (slope = D and Intercept = C) with a break point at some dielectric value. The user inputs the break point as well as the slope and intercept of each line.

As shown in Figure 5, this relationship can be generated in the laboratory during the optimum moisture content determination. A simple spreadsheet can automatically compute the values of C and D. Case Study 2 will provide an example.



Left Side: Open Metal Plate File

Right Side: Laboratory Generated Calibration Curves Relating Dielectric Values to Air Voids Content and Base Moisture Content.

Figure 11. Options Screen from RADAR2000.

Figure 12: Real-Time Display of Air Voids and Base Moisture Content

Similar to Figure 10, this figure shows the surface and base dielectric plots converted to HMA air void and base moisture contents using the calibration factors entered in Figure 11. To change the displays from dielectrics to air voids or base moisture, the user selects the %V or %M button at the top of Figure 10.

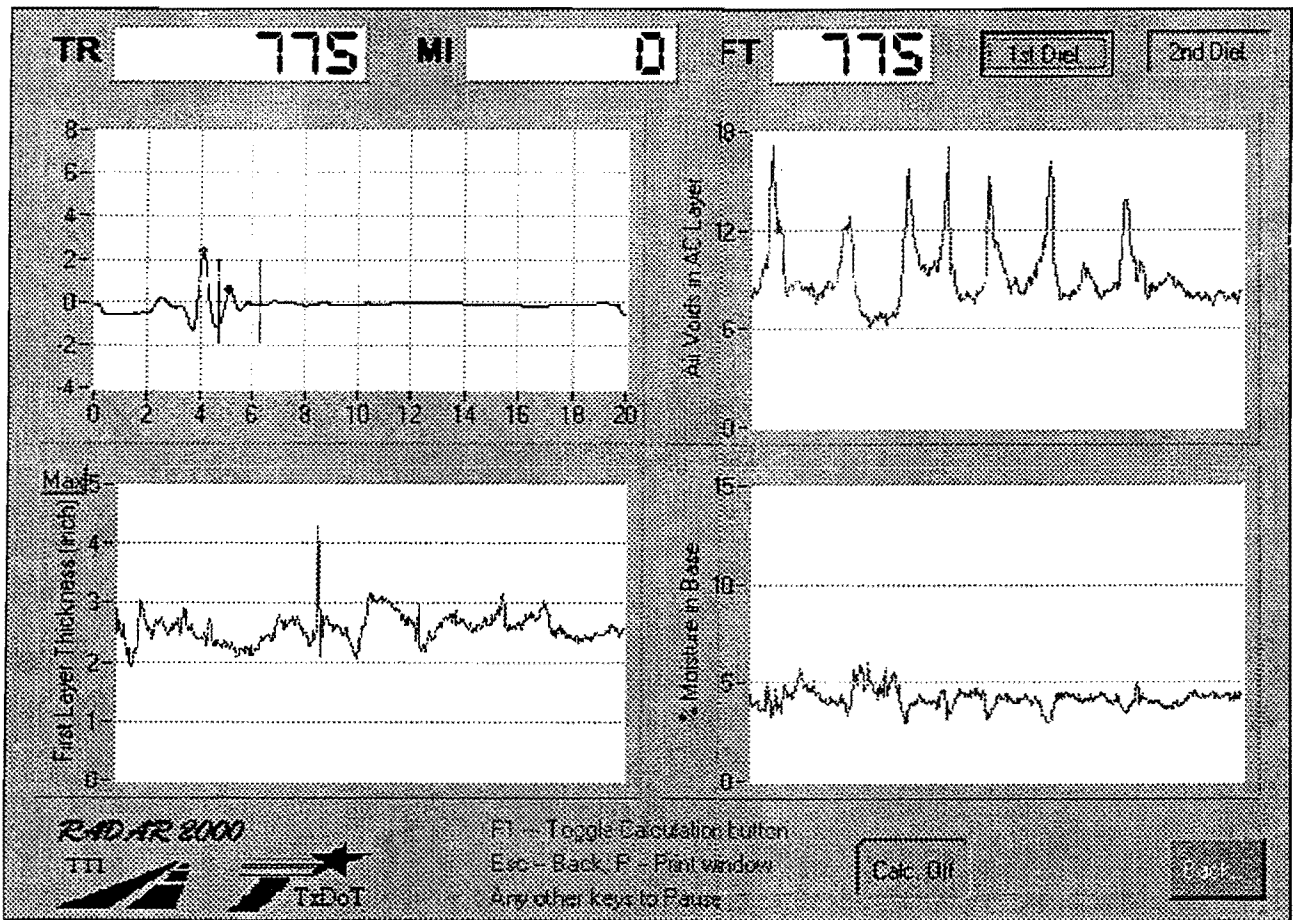


Figure 12. Real-Time Display of HMA Thickness, HMA Air Voids, and Base Moisture Content.

CHAPTER 3. CASE STUDIES

The RADAR2000 software has been used in a limited number of studies in Texas; two of these are described below. In both cases, the GPR data was collected while traveling at a speed of 15 to 20 mph with GPR traces collected at 1-foot intervals. In both cases, the real-time data processing feature was used to provide a continuous profile of subsurface conditions. The advantage of real-time processing is that it permits TxDOT to locate potential problem areas in the field. These problems areas may include locations where the overlay is too thin or where significant segregation or joint density problems are suspected.

CASE STUDY 1 SEGREGATION STUDIES ON IH 20

Segregation is a major problem in new overlays in Texas. It is observed as areas where the asphalt material has a coarser structure. These areas are more prone to rutting and cracking and have increased permeability which may permit moisture to enter into the lower structural layers. Segregated areas are frequently focal points for pavement deterioration. The types of segregation, their causes, and potential remedies have been under investigation for many years. What has always been missing is a convenient method of identifying and quantifying these problem areas in the entire mat, particularly shortly after material placement. With some dense graded mixes, the problem is visually apparent immediately after lay down, but with coarser materials, the problems are not apparent until after several months in service. Ground Penetrating Radar technology and the RADAR2000 data processing system show potential to assist in defining the severity of the segregation problem and in evaluating the effectiveness of remedial changes in construction practices.

The site used in this study was a section of IH 20 in the Odessa District. The District placed two different mixes and wanted to investigate if GPR could be used to compare their finished surfaces. The first mix was a traditional TxDOT dense graded Type B material. The second was an experimental large stone Superpave mix. Both materials were to be used as part of a mill and inlay operation and both were covered with a 1.5 inch surface course. The GPR testing was done shortly after placement of the two materials but prior to the placement of the final surface.

The construction process used to place both materials is shown in Figure 13. The HMA is first “belly dumped” in a wind-row in front of the paver. The material is then picked up and remixed prior to feeding it into the paver. A combination of steel wheel and pneumatic rollers performed compaction. The District Construction Engineer, Mr. Steve Smith, PE., speculated that these commonly used construction techniques may be prone to introduce significant temperature segregation, particularly at the tapered end of the load, which cools rapidly before the next load is placed. The GPR data collection and analysis discussed below were part of a larger study in which both GPR and infrared video images were recorded. The infrared images clearly demonstrated that temperature segregation was occurring with these materials and construction practices.

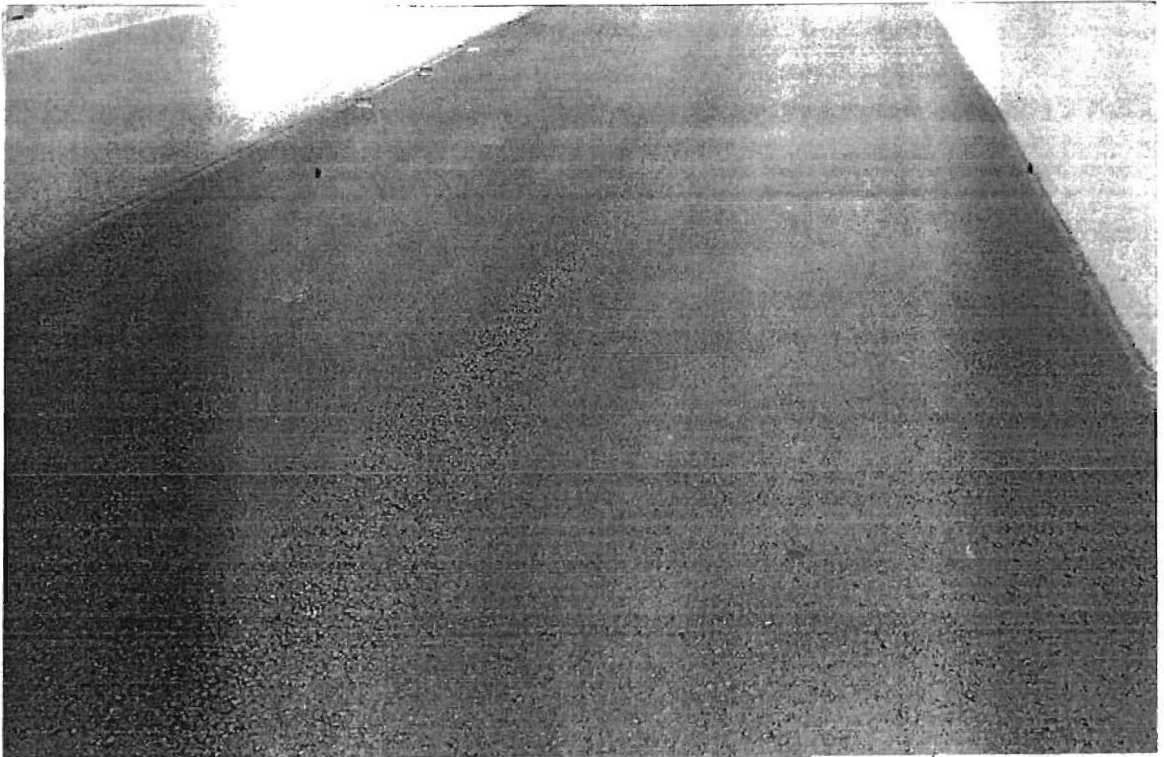
Figure 14 shows visual evidence of segregation in the Type B material one week after placement. In Figure 14(a), the area of concern is the strip down the center of the lane. In Figure 14(b) the problem appears to be localized in the inner wheel path. GPR data was collected over the entire 11-mile project with one trace collected for every foot of travel in the outer wheel path. Two representative 1500-foot study areas were then identified for the Type B and Superpave materials. The GPR unit passed over each of these sections five times at different transverse locations (outer edge, outer wheel path, middle, and inner wheel path and inner edge). Figure 15 shows a representative GPR trace from the Superpave material. After surface removal, the reflections from the top of the old HMA and top of the granular base are clearly present. In evaluating the uniformity of the material, the reflection of major importance is reflection A from the surface of the material. Using the RADAR2000 package, researchers computed the variation in the surface dielectric for both materials. Figure 16 shows representative sets of data. Both the Superpave and the Type B material have significant periodic drops in surface dielectric. In the Type B material, these drops in dielectric coincided with the visually segregated areas in the HMA layer. The surface dielectric is relatively constant for the dense graded mix between the segregated areas. The Superpave is a coarser mix, and the natural variations in its surface dielectric are greater than the Type B mix. However, significant dips in surface dielectric are also present in the Superpave material even though the segregated areas were much more difficult to detect visually. Due to construction constraints, no additional coring or validation was possible on these sites. This project received a chip seal and a thin overlay the day after GPR testing.

Figure 17 shows a representative plan view of this site. This site plan was developed based on the 5 GPR passes made over the test area. The dark areas represent areas with a significant decrease in surface dielectric. The inside wheel path contained the majority of the problems.



Figure 13. Lay Down Operation Large Stone Superpave Mix on IH 20.

(a)



(b)

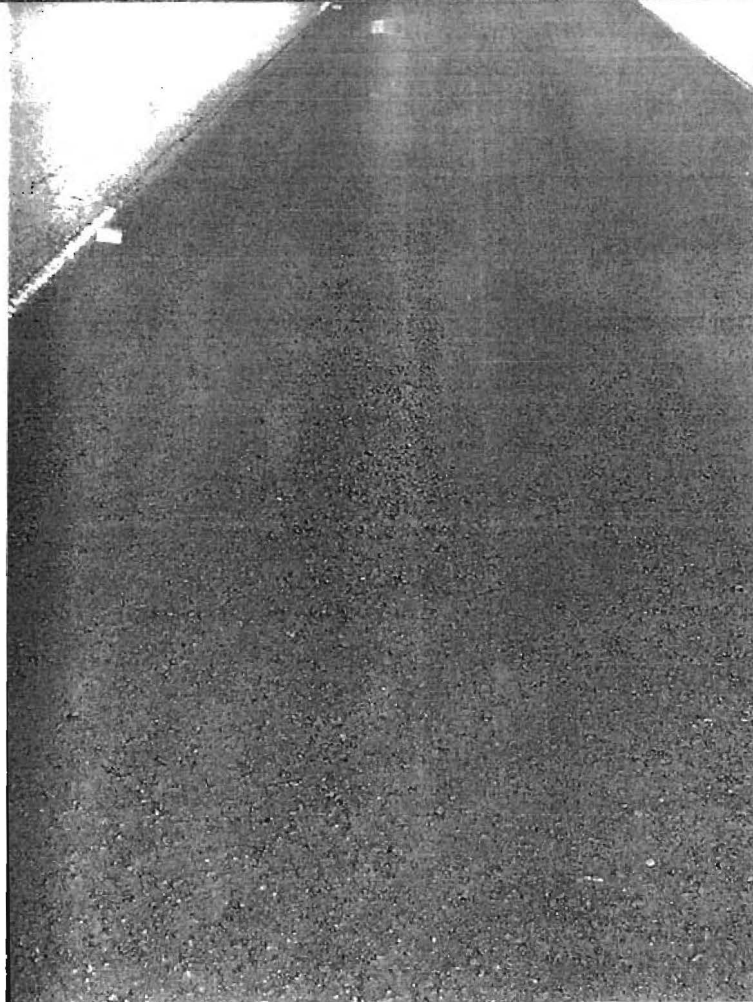
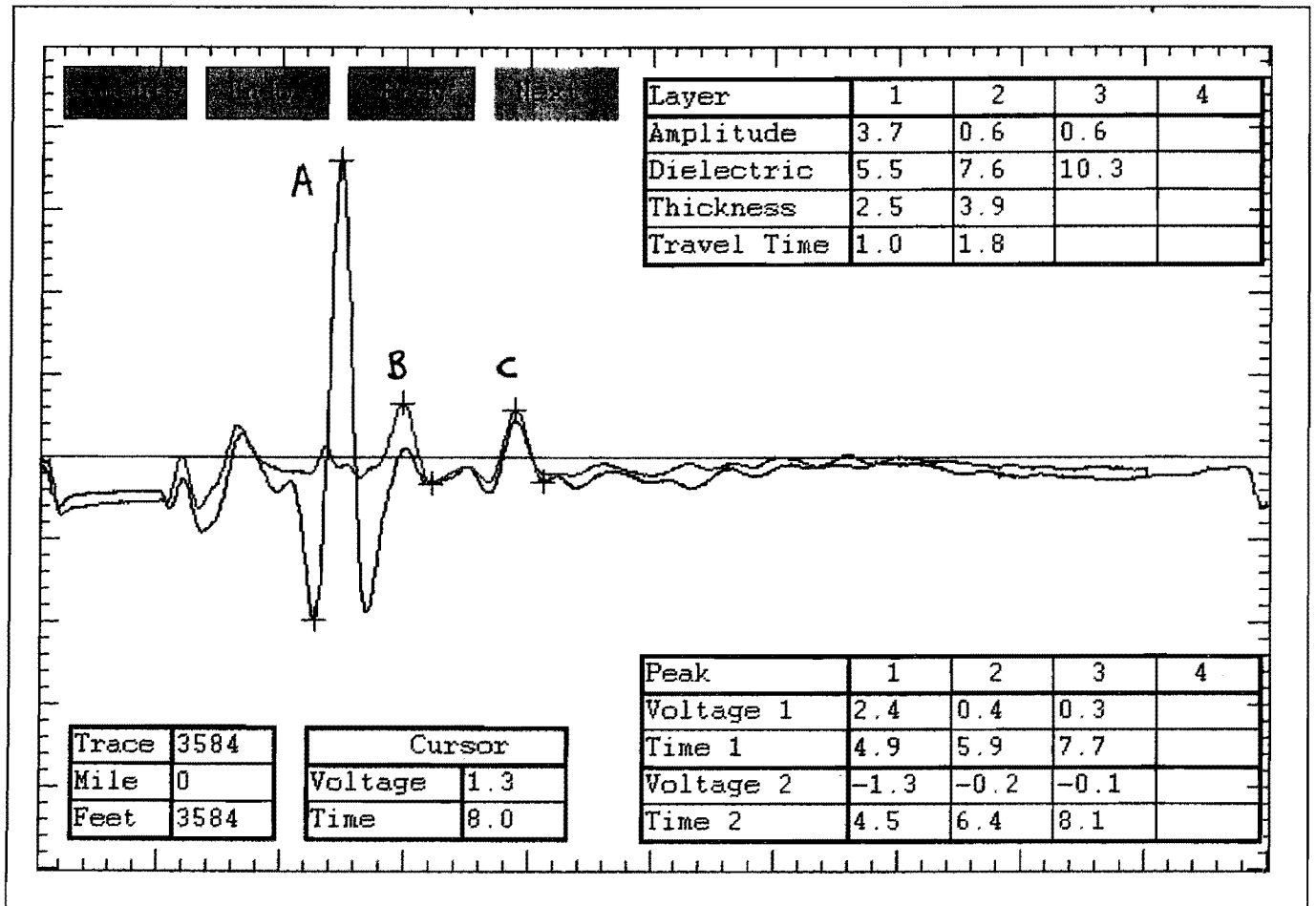


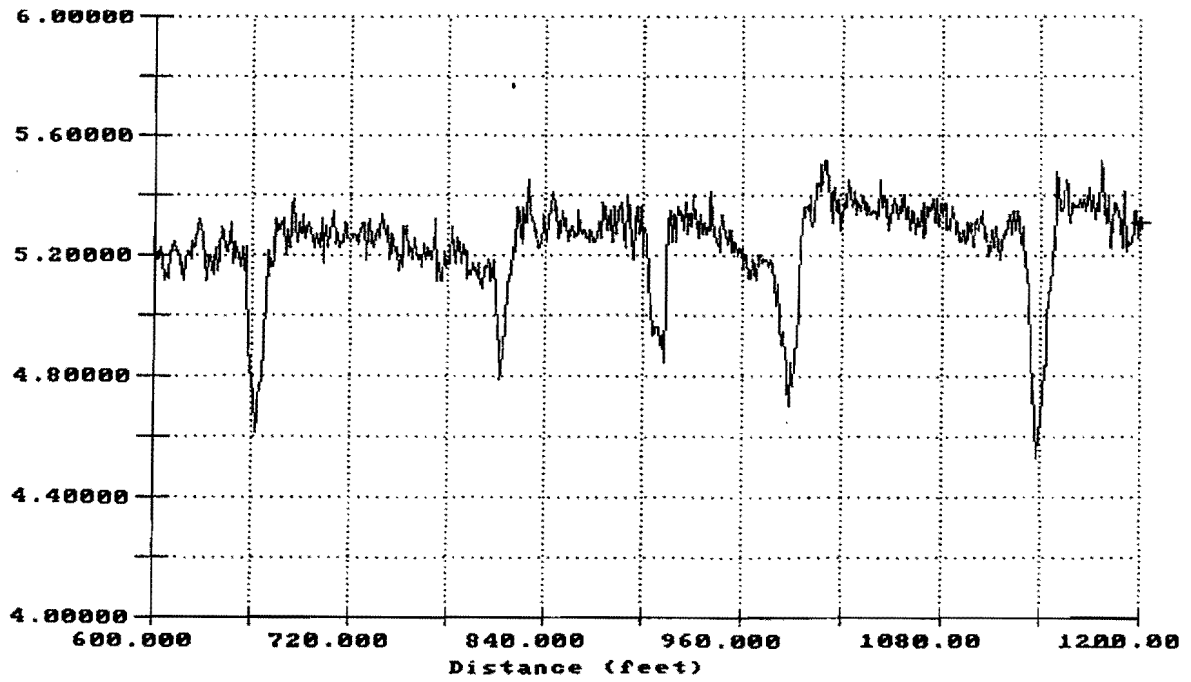
Figure 14. Evidence of Visual Segregation in Type B Material (One Week After Placement).



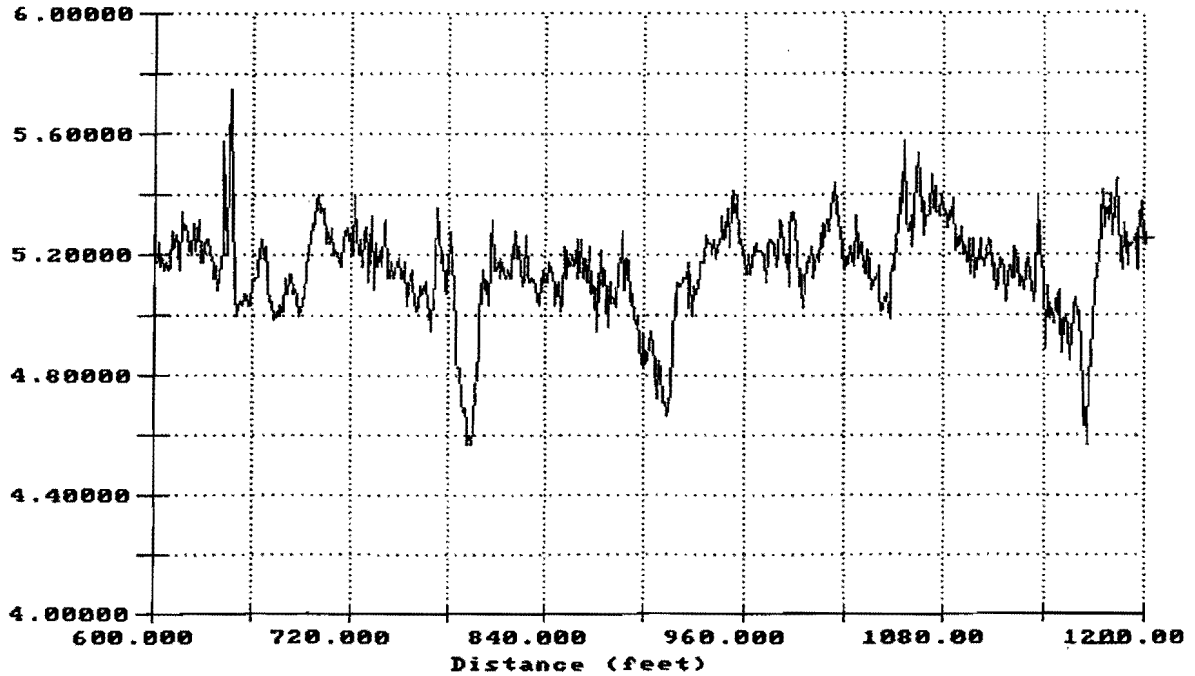
- A. Reflection from Surface
- B. Reflection from Top of Old HMA
- C. Reflection from Top of Base

Note: A significant reduction in amplitude A indicates a location of reduce density.

Figure 15. Typical GPR Trace from Superpave Inlay on IH 20, Odessa.

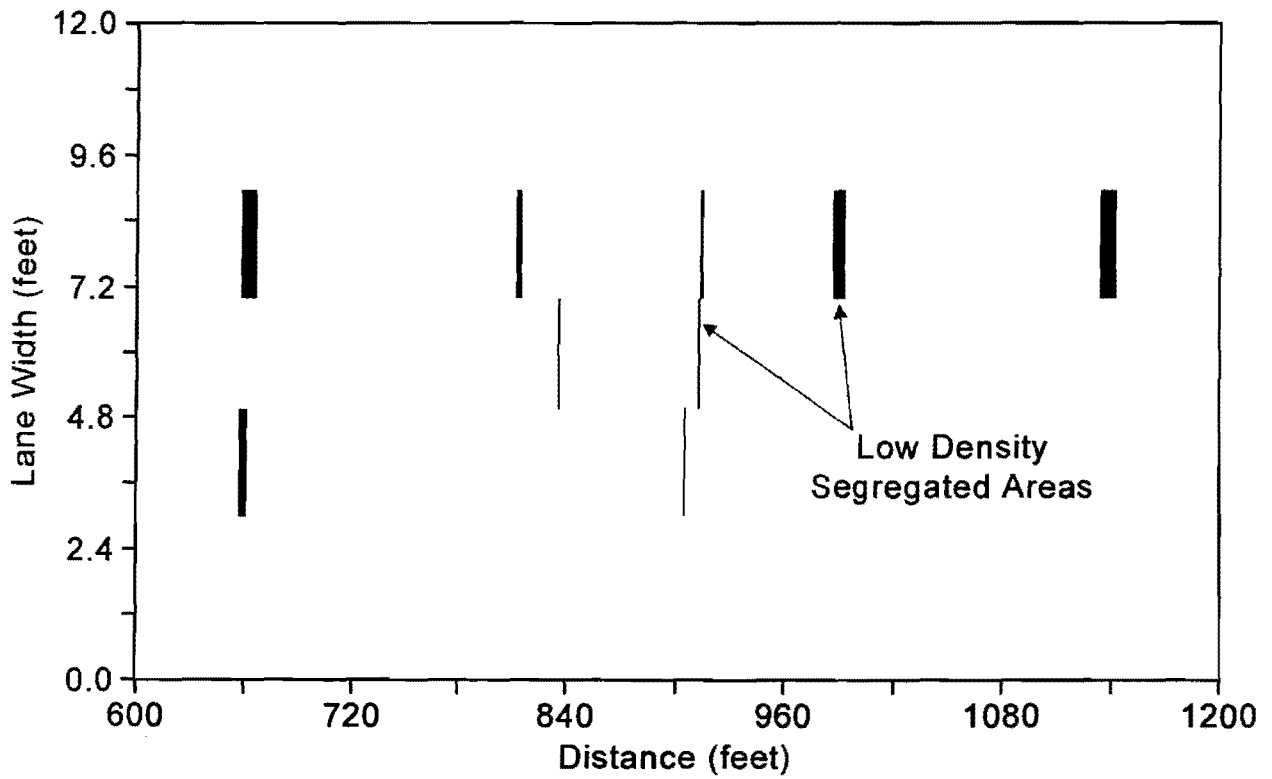


(a) Superpave 25 mm Mix



(b) TxDOT Type B Mix

Figure 16. Surface Dielectric Plots for Superpave vs. Type B Materials (Computed Surface Dielectric vs. Distance).



Plan View of Type B Mix Laid on IH 20 in Odessa District
 July 1999

Figure 17. Summary GPR Results from Type B Material.

CASE STUDY 2 POORLY COMPACTED LONGITUDINAL CONSTRUCTION JOINT

Researchers performed this GPR investigation as part of a forensics study to identify the cause of rapid failure of a newly constructed section of Interstate pavement. At the time the failure occurred, the structure consisted of 2.0 inches of HMA over a thick granular base. The final structure was to receive additional HMA, but traffic was placed on the section to facilitate construction of an adjacent lane. Shortly after opening to traffic, failures developed close to a longitudinal construction joint. Figure 18 shows the suspect construction joint as well as a close-up of a failed section.

Field-testing consisted of GPR testing in which both the lanes and construction joint were tested. The GPR vehicle drove in a zigzag fashion along the section while testing the construction joint. The RADAR2000 output illustrating the GPR results for several passes over the joint is shown in Figure 19. The information of major significance is the surface dielectric plot shown in the upper right hand box. Each time the GPR unit passed over the longitudinal construction joint, the surface dielectric decreased markedly. Away from the joint, the dielectric measured between 5.5 and 6, whereas over the joint the value ranged from 4 to 4.5.

In order to relate the dielectric to air void content, cores were taken for laboratory calibration. Samples of both the flexible base and HMA surfacing were recovered for lab calibration. Two cores were taken from the HMA layer, one in the middle of the lane and the second next to the longitudinal joint. At the first location, the surface dielectric was computed to be 5.5 and the air voids measured at 7.9%. Near the joint, the computed dielectric was 4.1 and the measured air voids were 16.8%. The form of the assumed relationship between air void constant was shown earlier in Figure 6; it is repeated below:

$$\% \text{ Air Voids} = A \times \exp. (- B \times \epsilon)$$

where A and B are constants determined from calibration cores
 ϵ is the surface dielectric as measured by the GPR unit

With the lab air voids vs. field dielectrics given above, the values of $A = 152.3$ and $B = 0.538$ were computed.

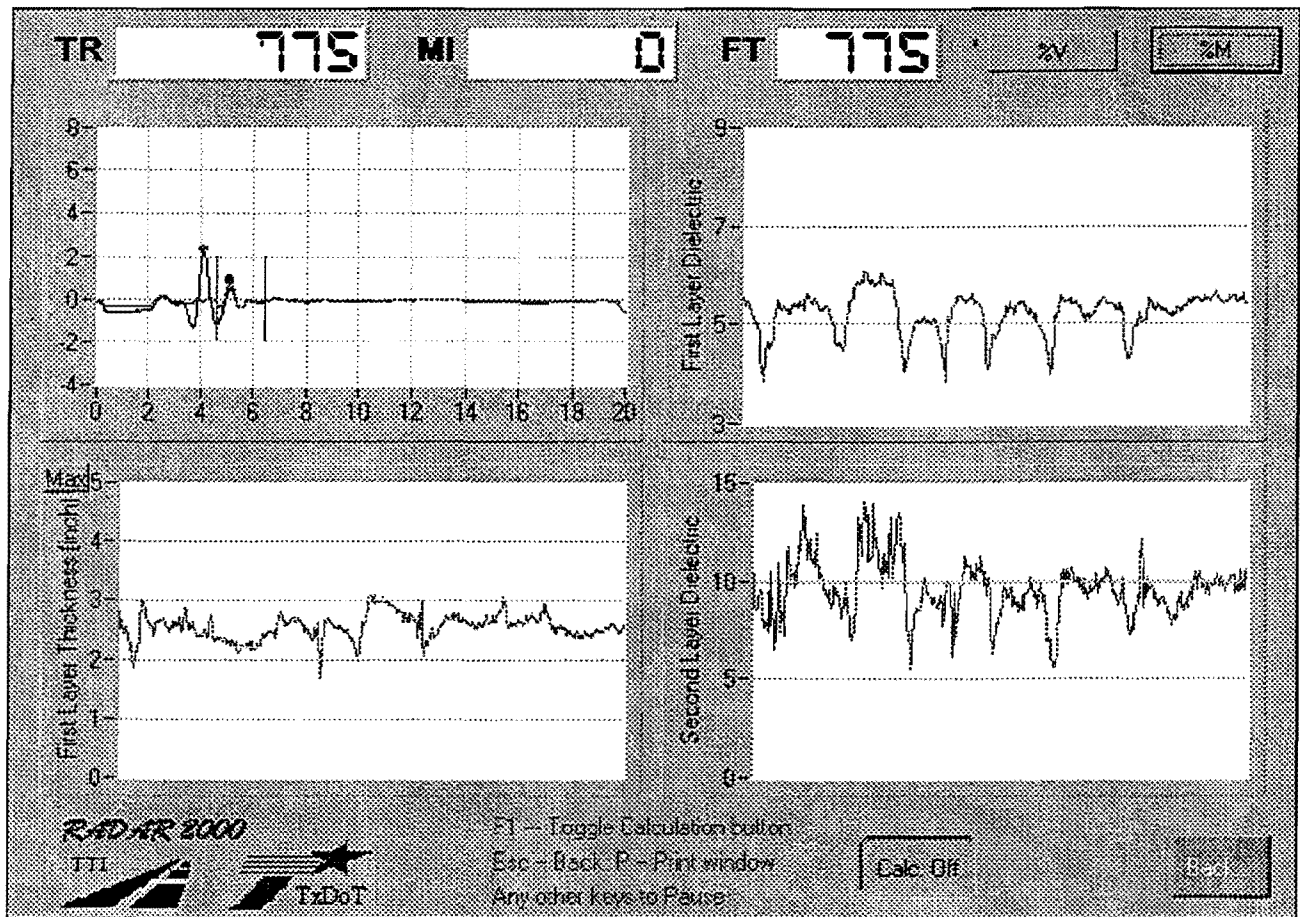


(a) Suspect Longitudinal Joint.



(b) Failed Section Which Occurred Either Side of Longitudinal Joint.

Figure 18. Forensic Evaluation on IH 20.



The significant drops in first layer dielectric (upper right) were recorded at the joint locations.

Figure 19. GPR Results Taken Over Longitudinal Construction Joint on IH 20.

Samples of the flexible base material were also tested in the laboratory using the test procedure shown earlier in Figure 5. Figure 20 illustrates the relationship between surface dielectric and laboratory moisture content. This data does not show a distinct change in slope as the moisture content increases. The optimum moisture content for this material was around 8%. Above the optimum value there appears to be a slight change in the slope of the curve. Consequently, using the model described in Figure 5, a dielectric break point of 15 was selected. Below 15, the slope and intercept values are 0.52 and 0.0, respectively, above 15, the values are 0.36 and 2.41. The calibration factors for both air voids and moisture content determination were input into RADAR2000. Once the laboratory-determined calibration factors were available, it was possible to convert the computed surface and base dielectrics in air voids and base moisture content. This computation is shown in Figure 21. The upper right box contains the estimated air void content for the HMA layer. It clearly shows dramatic increases in air void content at the longitudinal construction joint. In this study it was concluded that the cause of the rapid pavement failure was the poor construction joints which permitted moisture to enter the lower base layers.

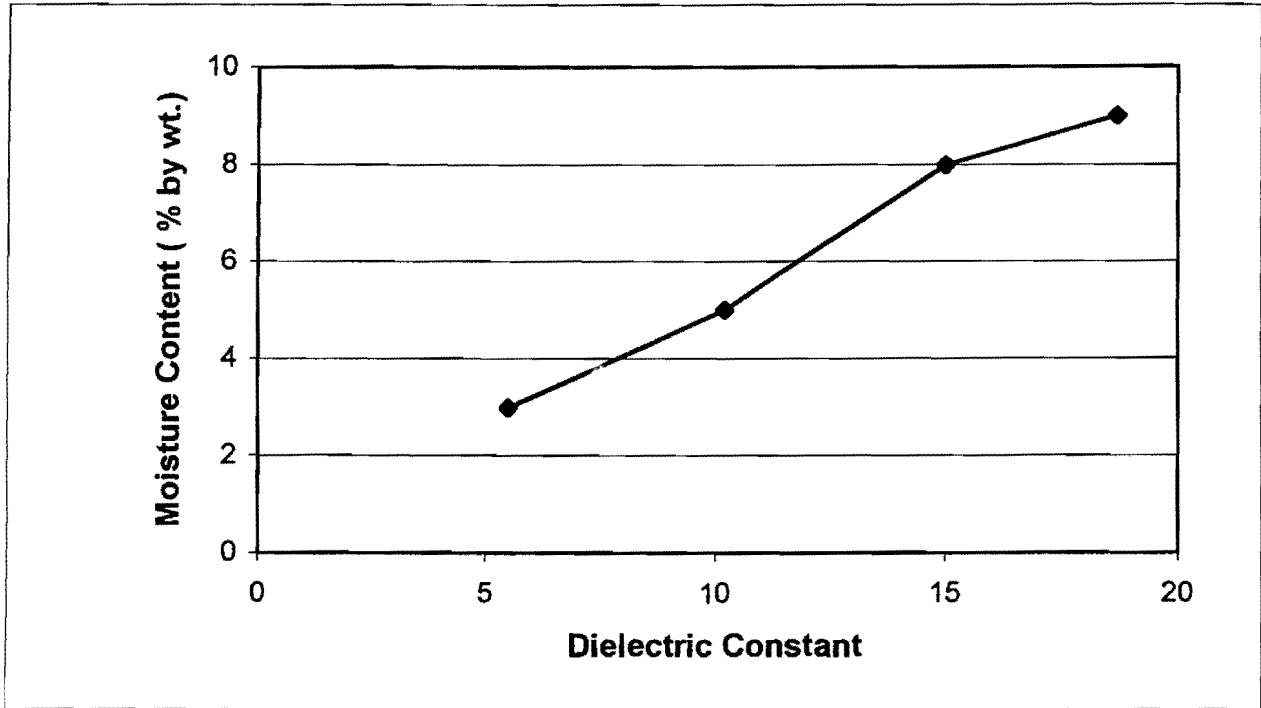


Figure 20. Laboratory Calibration Curve for the Base Material, Dielectric, as Measured with the Adek Probe, to the Moisture Content.

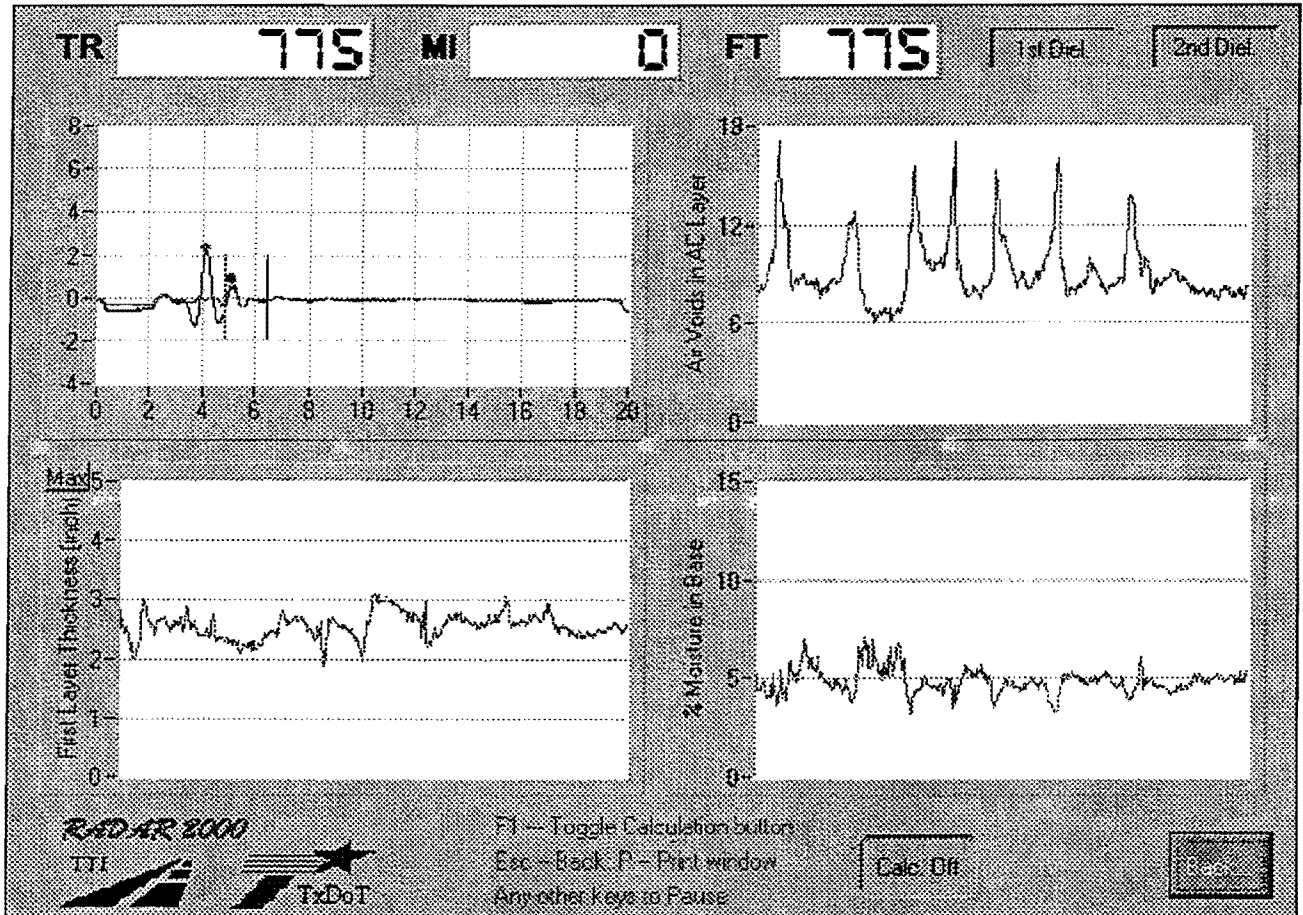


Figure 21. Using the Lab Calibration Factors to Estimate HMA Air Void and Base Moisture Content for IH 20.

CHAPTER 4. CONCLUSIONS AND RECOMMENDATIONS

This project developed a GPR data collection and processing system to be used in the field when evaluating the uniformity of thin HMA overlays. The system has the capability of computing in real-time the HMA layer thickness, HMA layer dielectric, and base layer dielectric. The HMA layer dielectric is correlated to air void content; significant reductions in dielectric are related to increases in air voids. A model and calibration procedure have been proposed in this study to convert field-determined dielectrics into HMA air void contents. The computed dielectric of the granular base layer is related to the moisture content of that layer. In this study, a model and laboratory calibration procedure have been proposed to convert field-measured dielectrics into base moisture contents.

With any development such as this, it is essential to clearly state the assumptions involved in the work. To perform QA/QC studies, it is essential to use stable GPR equipment with repeatable signals. Suitable GPR performance specifications have been developed by TTI for TxDOT (Scullion, Lau, and Chen 1992). Furthermore, the data processing system must account for antenna bounce as the vehicle travels over the section, and for thin surfacings signal de-convolution techniques must be applied. The model and calibration procedure proposed for air void determination have the following assumptions:

- The HMA surface is dry at the time of GPR testing. If the GPR data is collected shortly after significant rainfall, then the lower density areas may hold moisture. This will cause an increase rather than decrease in surface dielectric.
- Variations in asphalt content will have little impact on measured dielectric.
- Until more data is collected, the calibration procedure to develop the relationship between air voids and field dielectric value must be used on every job.

The model and calibration procedures used for the base moisture content determination include the following assumptions:

- The thin HMA layer will not significantly attenuate the GPR signal; laboratory test results at TTI show that this is reasonable for HMA material.

- The thin HMA layer will not significantly attenuate the GPR signal; laboratory test results at TTI show that this is reasonable for HMA material.
- There is a direct correlation between the dielectric value measured in the laboratory using the Adek, Ltd. (Plakk, 1994) dielectric probe and that computed using the GPR system. The two devices operate at different frequencies; the Adek probe's frequency is 50 KHz, whereas the GPR unit operates at 1 GHz. Limited fieldwork has been done to validate this assumption. However, studies conducted by Berthelot and Sparks (1998) found the assumption to be reasonable for Canadian base materials.
- Moisture variation is the only factor which will cause a significant increase in base dielectric. Variations in density of the base will have a minor impact on calculated dielectric.

Further studies are needed to validate this methodology. Control studies should be conducted with different HMA and base materials. The ideal approach would be to first test the pavement in the field with the GPR system, then review the results and identify locations of different surface dielectrics for coring and sampling. For the HMA layer, cores should be taken at a minimum of two locations for each job: where the mat appears to be normal and in areas where significant reductions in dielectric are observed to occur.

REFERENCES

1. Berthelot, C.F., and Sparks, G.A. (1998), "Ground Penetrating Radar Evaluation of Typical Saskatchewan Low Volume Road Soils," Report prepared by Vemax, Inc. for the Saskatchewan Department of Highways and Transportation.
2. Halabe, U.B., Maser, K., and Kausel, E. (1989), "Condition Assessment of Reinforced Concrete Using EM Waves," Final Report prepared for the US Army Research Office under contract DAAL 03-87-K005, Massachusetts Institute of Technology, Cambridge, Mass.
3. Maser, K., and Scullion, T. (1991), "Use of Radar Technology for Pavement Layer Evaluation," Second International Symposium on Pavement Response Monitoring Systems for Roads and Airfields, Sept. 9 – 12th, 1991.
4. Plakk, T., *HF Permittivity Measurements by Capacity Probe: User's Manual*. Adek, Ltd., Estonia, 1994.
5. Saarenketo, T., and Scullion, T. (1995), "Using Electrical Properties to Classify the Strength Properties of Base Course Aggregates," Texas Transportation Institute, Report 1341-2, Texas Transportation Institute, College Station, Texas, Nov. 1995.
6. Saarenketo, T. (1996), "Using GPR and Dielectric Probe Measurements in Pavement Density Quality Control," Transportation Research Board Record 1997, pp. 34-41.
7. Saarenketo, T., and Roimela, P. (1998), "Ground Penetrating Radar Techniques in Asphalt Pavement Density Control," Proceedings of the Seventh International Conference on Ground Penetrating Radar, May 27 – 30, 1998, Lawrence, Kansas, Vol. 2, pp. 461-46.
8. Scullion, T., Lau, C.L., and Chen, Y. (1992), "Implementation of the Texas Ground Penetrating Radar System," Texas Transportation Institute, Report 1233-1, College Station, Texas, Nov. 1992.
9. Scullion, T., Chen, Y., and Lau, C.L. (1995), "COLORMAP – User's Manual with Case Studies," Texas Transportation Institute Report, 1341 –1, College Station, Texas, Nov. 1995, 1341-1.